The rates of introgression and barriers to genetic exchange between hybridizing species: sex chromosomes vs. autosomes

Christelle Fraïsse[1,*] and Himani Sachdeva[1,2]

April 12, 2020

1. Institute of Science and Technology Austria, Am Campus 1, Klosterneuburg 3400, Austria
2. Mathematics and BioSciences Group, Faculty of Mathematics and Max F. Perutz Laboratories, University of Vienna, Vienna, Austria

* *Author for correspondence*: christelle.fraisse@ist.ac.at

Abstract

Interspecific crossing experiments have shown that sex chromosomes play a major role in the reproductive isolation of many species. However, their ability to act as reproductive barriers, which hamper interspecific genetic exchange, has hardly been evaluated quantitatively in relation to autosomes. Yet, this genome-wide limitation of gene flow is essential for understanding the complete separation of species, and thus speciation. Here, we develop a mainland-island model of secondary contact between hybridizing species of a XY (or ZW) sexual system. We obtain theoretical predictions for the frequency of introgressed alleles, and the strength of the barrier to neutral gene flow of the two types of chromosomes carrying multiple interspecific barrier loci. Theoretical predictions are obtained for scenarios where introgressed alleles are rare. We show that the same analytical expressions apply for sex chromosomes and autosomes, but with different effective parameters. The specific features of sex chromosomes (hemizygosity and absence of recombination in the heterogametic sex) lead to reduced levels of introgression of the X (or Z) compared to autosomes. This effect is enhanced by certain types of dosage compensation or sex-biased forces; but it remains overall small (except when incompatibilities are recessive). We discuss these predictions in light of empirical data comprising model-based tests of introgression and cline surveys in various biological systems.

Keywords

Speciation; gene flow; sex chromosomes; modelling

Running title

Multilocus sex-linked barriers to introgression

Introduction

Speciation is a process of gradual accumulation of reproductive barriers in the genome, ultimately leading to a cessation of gene flow between groups of individuals forming distinct biological species (Wu, 2001). The impact of these barrier loci on the reduction of interspecific gene flow is a major concept for the study of speciation, as it allows the strength of reproductive isolation to be quantified as populations diverge (Roux et al., 2016).

Another major advance in the genetics of speciation has been the discovery, by interspecific crossing experiments, of two extremely robust patterns: (i) "Haldane's rule" (Haldane, 1922), i.e. in species with sex-specific reduced fitness of F1 hybrids, the affected sex is generally heterogametic; and (ii) the "large-X effect" (Dobzhansky, 1936), i.e. the disproportionate density on the X chromosome of barrier loci causing hybrid sterility or inviability. These "rules of speciation" (Coyne and Orr, 1989) suggest the existence of universal mechanisms associated with sex chromosomes that may promote speciation.

However, these two lines of research (quantifying the barrier strength vs characterizing the molecular basis of speciation) were conducted largely independently so far. In particular, studies that quantitatively estimate the strength of the barrier to interspecific gene flow (e.g. by cline analyses) do not generally ascribe how much of this barrier is due to specific chromosomes, as this information is mainly available only for model species (Payseur et al., 2018). As a consequence, the ability of sex chromosomes to act as barriers that impede interspecies gene exchange has been little evaluated quantitatively or in a systematic way.

The recent explosion of genomic data in the field of speciation has provided empirical evidence across a diversity of species with different sex chromosome systems (i.e. XY under male heterogamety, and ZW under female heterogamety; Bachtrog et al., 2014). Indeed, the presence of reproductive barriers along the genome reduces interspecific gene flow locally around each barrier locus, leading to a local increase of interspecific differentiation relative to the rest of the genome. This prediction has been widely used to scan genomes for regions that are abnormally differentiated between species, in search of loci involved in speciation. These studies collectively show a systematically stronger differentiation of the sex chromosomes (X or Z) compared to the autosomes (Presgraves, 2018), even when accounting for the higher rate of genetic drift on the sex chromosome due to its reduced effective population size. This indicates that sex chromosomes may play a leading role in the isolation of nascent species.

However, caution must be exercised when interpreting this pattern, as relative measures of differentiation (such as F_{ST}; Weir and Cockerham, 1984) are sensitive to the level of diversity within species, whether or not gene flow occurred during species divergence (Cruickshank and Hahn, 2014). Complementary approaches addressing this limitation come from simple summary statistics of absolute divergence (such as D_{XY}; Nei and Li, 1979), cline analyses (Barton and Hewitt, 1985) and speciation model inferences (Sousa and Hey, 2013); but they do not reveal clear-cut patterns (see Discussion and Table 3). However, this may be because such analyses have been carried out for few systems so far since absolute divergence is not informative for many kind of markers (SNPs, AFLPs, microsatellites), and considering the difficulties associated with dense spatial sampling, or accurately inferring migration rates in non-equilibrium models.

Two main mechanisms have been proposed to explain why sex chromosomes may be expected to be stronger interspecies barriers than autosomes. First, sex chromosomes may accumulate interspecific barrier loci faster than autosomes. The faster-X theory (Charlesworth et al., 1987) predicts that this would be the case if incompatible loci first appear as recessive beneficial mutations within species. This is because the hemizygosity of the sex chromosome, i.e. the fact that the heterogametic sex has only one copy of the sex chromosome, makes selection more efficient by unmasking sex-linked recessive mutations. Most theoretical and empirical works so far have been done on the faster-X theory; however, the empirical evidence in favor of greater efficacy of selection on the sex chromosome is mixed (Meisel and Connallon, 2013). Instead, other studies have suggested that the accumulation of slightly deleterious mutations may be a major cause of faster-X, especially in birds, where the variance of male reproductive success strongly decreases the effective size of the sex chromosome relative to autosomes, increasing the effect of genetic drift (Mank et al., 2010).

Another theory, which was initially dismissed but has recently returned to the limelight, is that barrier loci may occur

more readily on the sex chromosomes, because the absence of recombination between the X and the Y (or the Z and the W) makes them more susceptible to segregation conflicts in the heterogametic sex (e.g. Bachtrog et al., 2019). Since segregation distorters and their suppressors co-evolve independently within lineages (often leading to cryptic systems), their interactions in hybrids may cause incompatibilities (Frank, 1991; Hurst and Pomiankowski, 1991). This theory thus contrasts with the classical view that interspecies incompatibilities first appear within species as beneficial mutations (Presgraves, 2010).

The second mechanism does not require that sex chromosomes harbor more barrier loci than autosomes, but simply that they are more exposed to selection, such that sex-linked incompatibilities cause more deleterious effects in hybrids. This process has been formalized by the dominance theory (Turelli and Orr, 1995, 2000), which is also based on the hemizygosity of the sex chromosomes and assumes that most incompatible mutations act recessively in hybrids. However, it has been tested and confirmed by genetic manipulation experiments only in Drosophila (e.g. Llopart et al., 2018); and assessing its generality remains difficult due to the experimental challenge of measuring the dominance of mutations.

The present work aims to understand the role of sex chromosomes in the formation of new biological species by focusing on the enhanced impact of sex-linked reproductive barriers on the reduction of gene flow between hybridizing species (second mechanism), rather than on their rate of establishment during species divergence (first mechanism). Hereof, a major step forward was made by Barton and Bengtsson who modelled the introgression of incompatible autosomal genomic blocks between hybridizing species (Barton, 1983), and quantified their effect on the effective migration rate at a linked neutral marker (Barton and Bengtsson, 1986). With multiple barrier loci, Barton and Bengtsson demonstrated that neutral gene flow is only significantly reduced over most of the genome if the number of loci involved in reproductive isolation is large, such that any neutral marker becomes closely linked to at least one barrier locus. While they have shown that this result is little influenced by the position of the neutral marker along a given chromosome, the effect of being located on the sex chromosomes rather than on autosomes was not addressed.

Yet, for the above reasons, one may expect to see differences between the two types of chromosomes: the greater efficacy of selection against deleterious mutations in the heterogametic sex, and stronger hitchhiking on sex chromosomes (due to the absence of recombination in the heterogametic sex) are expected to reduce the rate of introgression of sex-linked neutral markers relative to autosomal ones, even when there is no difference between the number, density and selective effects of sex-linked and autosomal incompatibilities.

Moreover, because sex chromosomes are involved in sex determination, they are inherited differently between males and females and thus spend different periods of time in each sex, making them sensitive to sex-specific evolutionary forces (Hedrick, 2007), such as sex-biased migration, sex-biased selection or achiasmy (the absence of recombination in the heterogametic sex). Since these evolutionary forces determine the intensity of the barrier to gene flow (Barton and Bengtsson, 1986), their sex specificity must be taken into account in order to quantify the role of sex chromosomes in speciation.

An additional complication comes from the phenomenon of dosage compensation that has been found in many species with a degenerated sex chromosome (Mank, 2013). The degeneration of the Y (or the W) causes a dose difference between the sexes, and so sex-linked loci are transcribed half as much in the heterogametic sex. Dosage compensation then consists of restoring the ancestral dose for sex-linked loci in order to correct potential imbalances in the genetic networks involving proteins encoded by both the sex chromosomes and autosomes. Among the diversity of mechanisms that have evolved (Gu and Walters, 2017), some may lead to a stronger selection against hybrids, and thus should enhance the ability of sex chromosomes to act as interspecific barriers.

To date, only a handful of theoretical studies have examined the role of sex chromosomes in speciation. The dominance theory (Turelli and Orr, 1995, 2000) offered a simple explanation for the two 'rules of speciation', building upon the allopatric model of postzygotic isolation elaborated by Dobzhansky (1937) and Muller (1940). This seminal model involves deleterious epistasis between alleles at different loci (i.e., Dobzhansky-Muller incompatibilities, or DMIs).

In a model of parapatry, Hoellinger and Hermisson (2017) found that pairs of sex-linked DMIs are more easily main-

tained in the presence of interspecies gene flow than autosomal DMIs, especially in the presence of dosage compensation and/or male-biased migration. However, these studies do not explicitly quantify the long-term effect of interspecies barriers on neutral gene flow, and they are limited to the special case of pairs of DMIs. These incompatibilities are inherently easy to evolve between species and create strong selection against F1 and F2 hybrids, but they are ineffective in keeping species apart in parapatry (Lindtke and Buerkle, 2015; Barton and Bengtsson, 1986).

By contrast, Muirhead and Presgraves (2016) modelled the effect of a locally deleterious mutation (either intrinsically incompatible with the local genome, or extrinsically incompatible with the local habitat) on gene flow at a linked neutral marker. Under a weak migration/strong selection regime, they showed that selection against incompatible mutations reduces the flow of neutral markers more strongly on the sex chromosomes than on autosomes, the effect being greater when mutations are recessive.

While all these studies are in line with a reduced introgression probability of the sex chromosomes relative to autosomes, they are limited to single/pairs of barrier loci, even though speciation is a complex, and probably multigenic, process. Thus, it is essential to develop more realistic models that take into account the effect of coupling between multiple barrier loci. This can have important implications for predictions; for example, Barton (1983) showed that autosomal polygenic barriers were much more resistant to interspecific gene flow than those generated by a single barrier locus of same strength. In addition, these models provide predictions of introgression patterns along chromosomes, and thus are critical to interpreting current genomic data.

Here, we address this gap by extending previous multilocus predictions (Barton, 1983; Barton and Bengtsson, 1986) to the case of sex chromosomes. We introduce a model where chromosomes contain multiple interspecies incompatibilities, and we quantify (i) their frequency on sex chromosomes relative to autosomes in populations under migration-selection balance and (ii) the effect of selection against these incompatibilities on the neutral gene flow between two hybridizing species. Our aim is to understand (i) to what extent the particularities of the sex chromosomes (hemizygosity and lack of recombination in the heterogametic sex) affect their ability to hinder interspecific gene flow, and (ii) the influence of sex-biased processes and dosage compensation in various sexual systems (XY and ZW).

Model and methods

We consider both males and females. The homogametic sex carries two copies of the sex chromosome and two copies of each autosome; the heterogametic sex carries one copy of the sex chromosome and two copies of each autosome. We further assume that the sex chromosome of the heterogametic sex does not recombine along its entire length, and so the X (or Z) is fully hemizygous (i.e., no pseudo-autosomal region). Our model is thus general in the sense that it applies to both male heterogamy (males are XY, and females are XX) and female heterogamy (females are ZW, and males are ZZ), and it allows us to address various kinds of sex-specificity by introducing sex-specific parameters. Unless otherwise stated, we assume a XY system in the analysis, as results for a ZW system would be generally the same, swapping males and females.

Hybridisation between two incompletely isolated species occurs in a mainland-island setting. Migration is assumed to be one-way from a donor to a recipient species, although our results hold for two-way exchange as long as migration is weak and introgressed alleles are rare. We focus on the dynamics of a single medium-sized block of genome with multiple loci that influence fitness in the recipient species. We assume that the two species are fixed for different alleles at these loci, and that each introduced allele is deleterious in the recipient species, either because they are not adapted to the local environment or to the local genetic background. Throughout we neglect *de novo* mutations and segregating variants that may be private to one of the two species. By focusing on the dynamics of single blocks, we neglect the effect of loosely linked incompatible alleles. However, as these would typically be spread across the entire genome, they would affect introgression of both autosomal and X-linked blocks to the same extent *via* an increase in the fitness variation and a resultant reduction in the effective population size (Barton, 1995). We thus focus here on the comparison of the introgression dynamics of a single X-linked *vs* autosomal block.

In each generation, a fraction m_F of females and a fraction m_M of males are replaced by immigrant females and males respectively. Immigrants are drawn from a donor species which is fixed for the deleterious block. Thus, if the block is on the X, immigrant females introduce two copies and immigrant males a single copy into the recipient species; while if it is autosomal, any migrant carry two identical copies of the deleterious block (i.e., on both of their autosomes). The block is assumed to carry L equally spaced loci with deleterious alleles of equal effect, that multiplicatively reduce individual fitness in the recipient species. The per generation rate of recombination between adjacent selected loci is c_F in females and c_M in males. We introduce a neutral marker that lies at the end of the deleterious genomic block ("rod" model, Barton and Bengtsson, 1986). In this model, the neutral marker can thus escape into the recipient background via a single recombination event. The rate of recombination per generation between the neutral marker and the nearest selected locus is αc_F in females and αc_M in males. Note that on the sex chromosome, no recombination between the X and Y occurs in males (i.e. $c_M = 0$).

In our analytical framework, we assume that (i) the frequency of the introgressing block (and its descendant fragments) is low and so mating between individuals carrying introgressed material can be neglected; and (ii) the deleterious block is short enough that multiple crossovers within the deleterious block (during any one meiotic cycle) can also be neglected. This implies that any individual male or female carries at most a single deleterious block in the genome. If we consider immigrant females (who carry two copies of the selected blocks), they must necessarily pass on only one of these to any of their offspring (who is likely to inherit the other chromosome from a father bearing no introgressed material). Thus, to first order in selection coefficients, introgression depends only on the heterozygous selective effect per deleterious allele, which we denote by s_F and s_M in females and males respectively. A female or male carrying y introgressing alleles (either on an autosome or on the X chromosome) thus has relative fitness $v_F(y) = e^{-ys_F}$ and $v_M(y) = e^{-ys_M}$ respectively.

In the following sections, we derive analytical results at migration-selection balance for the steady state frequency of deleterious blocks of the introduced genomes (section 1), and for the effective migration rate of neutral markers into the recipient species, thus quantifying how much gene flow at a neutral marker is impeded due to linkage to interspecific barrier loci in steady state (section 2). We also confront these analytical expressions (i.e., exact formulas, and approximations for weak selection) with individual-based simulations (section 3). We first consider a basic model assuming co-dominance, multiplicative effects, no dosage compensation and no sex-specific forces; and then extend it by including sex-specificities, dominance and epistasis. Notation used in the model is summarized in Table 1.

Table 1. Notation

Note that throughout we use s to denote the heterozygote selective effect (unlike the more standard notation, where s refers to the homozygous effect). Our choice of notation is motivated by the fact that to first order in sL (where L is the number of selected loci on the block) introgression depends only on this single parameter and is independent of the dominance coefficient, h.

Parameters	Meaning
L	number of selected loci equally spaced on the genomic block
c_F, c_M	rate of recombination per generation between adjacent selected loci in ♀ (resp. ♂)
αc_F, αc_M	rate of recombination per generation between the neutral marker and the nearest selected locus
m_F, m_M	fraction of females (resp. males) in the recipient species replaced by migrant females (resp. males) in each generation
s_F, s_M	heterozygous selective effect per locally deleterious allele in females (resp. males)

Quantities	Meaning
$P_F(y)$; $P_M(y)$	fraction of females (resp. males) carrying a single introgressing block with y locally deleterious loci X CHROMOSOME: $P_X(y) = \frac{P_F(y)+P_M(y)}{3}$; AUTOSOME: $P_A(y) = \frac{P_F(y)+P_M(y)}{2}$
$\overline{p}_X$; $\overline{p}_A$	frequency of locally deleterious alleles on the sex chromosome (resp. autosomes) averaged over all selected loci
$\overline{u}_X$; $\overline{u}_A$	frequency of the neutral marker lying at the end of the sex chromosome (resp. autosomes) averaged over all deleterious backgrounds
b_X ; b_A	strength of the sex chromosomal barrier to neutral gene flow (resp. autosomal)

Model extensions	Meaning
h	dominance coefficient of the locally deleterious alleles
	$h = 0.5$: co-dominance; $h = 0.1$: partial recessivity; $h = 1.0$: complete dominance
$s_{hom,F} = \frac{s_F}{h}$; $s_{hom,M} = \frac{s_M}{h}$	homozygous selective effect per locally deleterious allele in females (resp. males)
$v_F(y, y')$; $v_M(y, y')$	fitness of a female (resp. male) carrying y locally deleterious loci in the heterozygous state and y' loci in the homozygous state
	X CHROMOSOME: $v_F(y, y') = e^{-ys_F - y's_{hom,F}}$, $v_M(y) = e^{-ys_M}$; AUTOSOME: $v_F(y, y') = e^{-ys_F - y's_{hom,F}}$, $v_M(y, y') = e^{-ys_M - y's_{hom,M}}$
β	fraction of selected loci that act epistatically, the remaining $1 - \beta$ acts multiplicatively
ε	direction and strength of epistasis
	$\varepsilon = 1$: multiplicativity; $0 \leq \varepsilon < 1$: negative epistasis

Table 2. Effective parameters

These effective parameters govern introgression at steady state assuming that sL, cL and m are $\ll 1$.

Parameters	Meaning
s_X ; s_A	effective heterozygous selection per locally deleterious allele on the X chromosome (resp. autosomes)
	X CHROMOSOME: $s_X = \frac{s_F + (s_M/2)}{2}$; AUTOSOME: $s_A = \frac{s_F + s_M}{2}$
m_X ; m_A	effective migration on the X chromosome (resp. autosomes)
	X CHROMOSOME: $m_X = \frac{m_F + (m_M/2)}{2}$; AUTOSOME: $m_A = \frac{m_F + m_M}{2}$
c_X ; c_A	effective recombination on the X chromosome (resp. autosomes)
	X CHROMOSOME: $c_X = \frac{c_F}{2}$; AUTOSOME: $c_A = \frac{c_F + c_M}{2}$
θ_X ; θ_A	strength of coupling between locally deleterious alleles on the sex chromosome (resp. autosomes)
	X CHROMOSOME: $\theta_X = \frac{s_X}{c_X}$; AUTOSOME: $\theta_A = \frac{s_A}{c_A}$
$\frac{m_X}{S_X}$; $\frac{m_A}{S_A}$	expected allele frequency when selected loci are perfectly linked on the sex chromosome (resp. autosomes)

1. Introgression of multilocus deleterious blocks

Autosomal introgression

We consider how selection against multiple deleterious alleles influences introgression of an autosomal block, in a regime where the vast majority of individuals in the population will carry at most one fragment of the incompatible block. While Barton (1983) considers the simplest case of haploid introgression and no sexes, we generalise this framework to the case where selection coefficients, migration rates and recombination rates are different across males and females, i.e., $s_F \neq s_M$, $m_F \neq m_M$ and $c_F \neq c_M$(see Appendix A). When these parameters are small (i.e. sL, cL, $m \ll 1$) and migration is weak compared to selection (i.e. $m \ll s$), the steady state frequencies $P_A(y)$ of introgressed fragments with y deleterious alleles, satisfy a simple set of equations, which are identical to those in Barton (1983) but with s_A, m_A and c_A given by the sex-averaged rates (see Table 2):

$$0 = -\left[s_A y + c_A(y-1)\right] P_A(y) + 2c_A \sum_{y'=y+1}^{L} P_A(y') + m_A \delta_{y,L} \tag{1}$$

where $\delta_{y,L}$ equals 1 for $y = L$, and is zero otherwise. In steady state, the rate of loss of any fragment due to selection and back-crossing with the recipient species (first term), is balanced by the rate at which it is generated by splitting of larger fragments (second term). For the full block (with L alleles), we must also include the contribution of migration from the donor species (third term). Note that eq. (1) is linear in $P_A(y)$, which again reflects the assumption that introgressing blocks are rare and terms of the form $P_A(y)P_A(y')$ (which arise from mating between two individuals carrying introgressing blocks) can be neglected. For this very reason, we can ignore terms of the form m_A^2, and thus our results for one-way migration also hold when migration is symmetric between the two species.

Eq. (1) can be solved recursively to obtain $P_A(y)$ (see eq. (11) in Appendix A). This can be used to calculate the

average frequency of deleterious alleles, averaged over all loci on the autosomal block: $\overline{p}_A = \sum_{y=1}^{L} P_A(y)\frac{y}{L}$. We define the effective selection, $s_A^* = \frac{m_A}{\overline{p}_A}$, as the selective pressure at a single locus that would be needed to produce the observed average frequency of the deleterious alleles (Barton, 1983). By extension, we can also define the effective number of loci $n_{eA} = \frac{s_A^*}{s_A}$, that, if fully linked, would have produced the same effect on deleterious allele frequency as the full deleterious block (Figure S1). Note that in the limit $c \to 0$, i.e., for perfect linkage between deleterious alleles, n_{eA} must approach L.

A key parameter governing introgression is $\theta_A = \frac{s_A}{c_A}$, the ratio of selective effect to recombination rate per allele, which determines the extent of coupling between loci (Barton, 1983). For large L, the average deleterious allele frequency $\overline{p}_A$ can be approximated as:

$$\overline{p}_A \sim \begin{cases} \frac{m_A}{S_A} L^{1-2\theta_A} & \theta_A \ll 1 \\ \frac{m_A}{2S_A}(0.577216 + \log[4L]) & \theta_A = 1 \\ \frac{m_A}{S_A}\left(1 + \frac{1}{\theta_A}\right) & \theta_A \gg 1 \end{cases}$$

For $\theta_A \gg 1$, (i.e., very strong coupling between loci), the deleterious allele frequency depends only on the net selective disadvantage $S_A = s_A L$ of the block, and is independent of the number of loci that the block carries (for large L). It also follows that the effective selection against each individual locus, given by $S_A/(1 + \frac{1}{\theta_A})$, increases as the coupling between loci becomes stronger, and approaches the net selective effect S_A for very large values of θ_A.

For $\theta_A \ll 1$ (i.e., weak coupling between loci), each locus experiences an effective selective disadvantage (given by $S_A L^{2\theta_A - 1} = s_A L^{2\theta_A}$) which is proportional to its own selective effect s_A, but also depends weakly on L (the number of selected loci that are loosely linked to it). Crucially, in this regime the effective selection per locus decreases, and the deleterious allele frequency increases, as we consider introgression scenarios where the same total selective effect is due to a larger and larger number of loci of weaker effects (i.e, as we increase L, keeping $S_A = s_A L$ and $C_A = c_A L$ constant). Thus for weak coupling between loci, this analysis (which assumes that deleterious allele frequency is low) remains valid only for small values of L, more specifically as long as $\frac{m_A}{S_A} L^{1-2\theta_A} \ll 1$.

X-linked introgression

We now turn to the case where the introgressing block is X-linked. We use $P_F(y)$ and $P_M(y)$ to denote the steady state fraction of females and males who carry a single copy of an X-linked introgressed block (with y deleterious alleles). This implies that in a population of size N with a $1:1$ sex ratio, the number of X-linked blocks with y deleterious alleles is $\frac{N}{2}(P_F(y) + P_M(y))$, while the total number of X-chromosomes is $\frac{3}{2}N$. Thus, the frequency of X-linked introgressed blocks with y deleterious alleles is given by $P_X(y) = \frac{P_F(y)+P_M(y)}{3}$. In Appendix A, we derive equations for the evolution of $P_F(y)$ and $P_M(y)$, and then use these to arrive at a set of recursive equations, which allow us to express the steady state frequency of any block in terms of the frequencies of larger parental blocks that contain it. Assuming that sL, $cL \ll 1$, and that $m \ll s$, these equations are:

$$0 = -\left[\frac{s_F}{2}y + \frac{s_M}{4}y + \frac{c_F}{2}(y-1)\right] P_X(y) + c_F \sum_{y'=y+1}^{L} P_X(y') + \left(\frac{m_F}{2} + \frac{m_M}{4}\right)\delta_{y,L} \tag{2a}$$

$$P_F(y) = 2P_X(y) \qquad P_M(y) = P_X(y) \tag{2b}$$

This equation is identical in form to eq. (1) (which describes the steady state distribution of autosomal blocks), but with s_A replaced by $s_X = \frac{s_F}{2} + \frac{s_M}{4}$, m_A by $m_X = \frac{m_F}{2} + \frac{m_M}{4}$ and c_A by $c_X = \frac{c_F}{2}$ (see Table 2). The composite selection coefficient s_X and composite migration rate m_X are weighted sums of male and female contributions: male migration contributes half as much as female migration to the composite migration rate m_X simply because female migrants carry two X-linked blocks while males carry one. The composite selection coefficient s_X is also the sum of male and female components: the contribution of s_M, the selective effect per allele in males, is half that of s_F, because half as many males

are heterozygous for any introgressed blocks as females (eq. (2b)). Thus any X-linked deleterious allele spends twice as much time in females as males. Note that $P_M(y) \sim \frac{P_F(y)}{2}$ does not imply that females carry two copies of introgressed X-linked blocks, since introgressed blocks are rare and typically present on a single X chromosome in females as well. Instead, the block frequency in males is half that in females simply because females can inherit the block from either parent, while males only inherit it from their mothers. Equation (2a) can be solved (details in Appendix A) to obtain an explicit expression for $P_X(y)$:

$$P_X(L) = \frac{m_X}{s_X}\frac{\theta_X}{(L-1)+\theta_X L}, \qquad P_X(y) = 2\frac{m_X}{s_X}\frac{\prod_{i=1}^{L-y-1}[\theta_X(y+i)+(y+i+1)]}{\prod_{i=0}^{L-y}[\theta_X(y+i)+(y+i-1)]}\theta_X \quad y < L \tag{3}$$

Here $\theta_X = \frac{s_X}{c_X}$ is a measure of the strength of coupling between deleterious alleles on the X chromosome. Equation (3) can be used to calculate the average frequency of deleterious alleles, averaged over all loci on the X chromosome: $\overline{p}_X = \sum_{y=1}^{L} P_X(y)\frac{y}{L}$. Since eq. (1) and (2) have the same form, the expressions for $P_X(y)$ and $P_A(y)$ must also be identical in form, with s_X and m_X replaced by s_A and m_A respectively. As in the autosomal case, we expect our analysis to become inaccurate when the X chromosome contains a large number of weakly linked and weakly selected deleterious alleles, i.e., for $\theta_X \lesssim 1$ and $\frac{m_X}{S_X}L^{1-2\theta_X} \ll 1$.

Equations (1) and (2) show that there is a simple correspondence between introgression on autosomes and X-linked introgression, even when there is multi-locus selection against introgression (for weak selection and recombination: $sL, cL \ll 1$). More specifically, they suggest that the distribution of lengths of X-linked introgressing blocks should be nearly identical to the distribution of autosomal introgressing blocks, as long as we compare autosomes and sex chromosomes with $\frac{m_X}{s_X} = \frac{m_A}{s_A}$ and $\theta_X = \theta_A$ (this pattern is confirmed in Figure S2). Conversely, if we compare autosomal and X-linked blocks with identical genetic architectures, then we have $\theta_X = \frac{3}{2}\theta_A$, i.e., deleterious alleles on the X are more strongly coupled to each other (than on autosomes), resulting in lower rates of introgression. We quantify this precisely in the Results using our analytical expressions for $P_X(y)$ and $P_A(y)$ (eq. (3)).

Dosage compensation, sex-biased forces and other model extensions

An important feature of the above equations is that any kind of sex bias can be encapsulated by the composite parameters $\theta = \frac{s}{c}$ and $\frac{m}{s}$, at least for weak migration, selection and recombination. Thus equations (2) and (3) describe X-linked introgression in various scenarios. We implement full dosage compensation by up-regulation of the X in males (i.e., $s_M = s_{hom,F} > s_F$ for sex-linked alleles), such that the fitness of a male carrying a hemizygous XY deleterious block drops down to that of a female carrying a homozygous XX block. Imbalance of the sex-linked gene dose can also be solved by down-regulation of the sex chromosome in the homogametic sex (XY system: $s_{hom,F} = s_M = s_F$, or ZW system: $s_{hom,M} = s_M = s_F$ for sex-linked alleles). In this situation, the fitness of a female carrying a homozygous XX deleterious block rises to that of a male carrying a hemizygous XY block. This second type of dosage compensation has no effect on introgression for sL, cL and $m \ll 1$ (see eq. (3)), as individuals carry at most one fragment of the deleterious block. We then model sex-specific selection on deleterious alleles by assuming stronger selection on XY males (i.e., $s_M > s_F$) or on ZZ males (i.e., $s_F > s_M$ in our XY notation). Finally, we study sex-biased migration by setting $m_M \neq m_F$; and achiasmy by setting $c_M = 0$ on autosomes in males, such that recombination between autosomes in XY males is null (or $c_F = 0$ in a ZW system).

We also consider various generalisations of the model. We first relax the assumption that selection against the introgressed block is weak (i.e., $sL \ll 1$): as we show below, in this regime, it becomes necessary to account for the effects of selection against deleterious alleles in the homozygous state (as in immigrant individuals), which are sensitive to the dominance coefficient of deleterious alleles (h). Even under these scenarios (i.e. strong selection and dominance/recessivity), we can write a set of linear equations for $P_F(y)$ and $P_M(y)$ as long as the frequency of deterious alleles in the recipient species is sufficiently low that second order terms in $P(y)$ can be neglected. These equations can be solved recursively,

i.e., by solving for $P_F(y)$ and $P_M(y)$ and then solving for $P_F(L-1)$ and $P_M(L-1)$ in terms of $P_F(L)$ and $P_M(L)$. In Appendix A, we present a general solution for $P_F(y)$ and $P_M(y)$, which is more accurate for strong selection against introgression. This expression is considerably more involved than the expression in eq. (3) above, and cannot be expressed in terms of the composite parameters (i.e. s_X, m_X, c_X). So, the simple correspondence between autosomal and X-linked introgression described above no longer holds under these model extensions.

We then consider the case where a fraction β of the loci act epistatically, and a fraction $(1-\beta)$ acts multiplicatively. Following Barton and Bengtsson (1986), the fitness of an individual with y introgressed alleles is then e^{-ay-by^2}, where $a = (1-\beta+\beta\varepsilon)s$, $b = \beta s(1-\varepsilon)$ and ε gives the direction and strength of pairwise epistasis (note that when $\beta = 0$, the fitness of an individual carrying a block with y equal-effect loci is $v(y) = e^{-ys}$). When $\beta > 0$ and $\varepsilon < 1$, selection acts more strongly against the locally deleterious alleles when they are numerous, i.e. there is negative epistasis.

2. Multilocus barrier to neutral introgression

Autosomal barrier

We next investigate the role of such deleterious genomic blocks as a genetic barrier to neutral gene flow by calculating the rate at which an allele at a linked neutral marker (fixed in the donor species) increases in the recipient species, where it is initially absent. We again assume that introgression is rare and that multiple crossovers within the deleterious block can be neglected. Therefore, the neutral marker can only be found in the recipient species associated with a consecutive series of between 0 and L locally deleterious alleles, and paired with a chromosome of the recipient species.

Following Bengtsson (1985), the strength of the barrier (b_A) is defined as $\frac{m_A}{me_A}$, where m_A is the raw migration rate on autosomes and me_A is the effective migration rate defined as $\frac{\delta u_A(0)}{\triangle u_A}$. Here, $\triangle u_A$ is the difference in allele frequency of the neutral marker between the donor and recipient species (and is 1, by definition), while $\delta u_A(0)$ is the rate of increase of the neutral marker in the recipient background. The rate of increase $\delta u_A(0)$ can be calculated by tracking the rate at which the neutral marker moves/migrates between different genetic backgrounds (with different numbers of deleterious alleles) in steady state (Barton and Bengtsson, 1986; see also Appendix B). There is a closed form solution for b_A (Barton and Bengtsson, 1986), which under the assumption of sL, $cL \ll 1$, can be written as:

$$b_A = \frac{\Gamma\left(L + \frac{\alpha+\theta_A}{1+\theta_A}\right)\Gamma\left(\frac{\alpha}{1+\theta_A}\right)}{\Gamma\left(L + \frac{\alpha}{1+\theta_A}\right)\Gamma\left(\frac{\alpha+\theta_A}{1+\theta_A}\right)} \tag{4}$$

The barrier strength is thus determined by the coupling coefficient ($\theta_A = \frac{s_A}{c_A}$) and the proximity of the neutral marker to the selected block (α). The dependence of the barrier strength on θ_A is qualitatively similar to the dependence of the steady state frequency of locally deleterious alleles (see section 1). When θ_A is large ($sL \gg cL$), all that matters for the neutral marker in order to introgress is to recombine away from the entire deleterious block in a single step; while when θ_A is small ($sL \ll cL$), the pairwise interactions between the neutral marker and each selected locus drive neutral introgression.

Concerning the closeness of the neutral marker to the incompatible block, the smaller is α, the stronger is the barrier, since the neutral marker is then closely linked to the block. When $\alpha \ll 1$, the barrier strength is proportional to the effect of the closest deleterious locus, but the additional effect of the other deleterious loci lying on the block reduces gene flow well below the single-locus expectation. When $\alpha \gg L$, the deleterious block act as a single unit with regard to the neutral marker, and thus the barrier strength is close to that produced by a single locus with total effect sL at a distance αc from the marker.

X-linked barrier

We now consider the case of a neutral marker lying on the X chromosome. By applying the same assumptions as in the autosomal case, we obtain a closed form solution for the strength of the barrier to neutral X-linked gene flow (see Appendix B for further details), assuming that sL, $cL \ll 1$:

$$b_X = \frac{\Gamma\left(L + \frac{\alpha+\theta_X}{1+\theta_X}\right)\Gamma\left(\frac{\alpha}{1+\theta_X}\right)}{\Gamma\left(L + \frac{\alpha}{1+\theta_X}\right)\Gamma\left(\frac{\alpha+\theta_X}{1+\theta_X}\right)} \tag{5}$$

As in section 2, an important feature of the above equation is that sex-specificities can be described by the composite parameter $\theta_X = \frac{s_X}{c_X}$.

3. Individual-based simulations

The key assumptions underlying the analytical expressions for the deleterious allele frequency (eq. (3) which assumes sL, cL and $m \ll 1$; eq. (15) in Appendix A which is also valid for strong selection) and for the barrier strength (eq. (5); eq. (29) in Appendix B) are the following: (i) we neglect drift (which is valid as long as Ns is reasonably greater than 1); (ii) we neglect multiple crossovers (which is valid as long as cL is reasonably smaller than 1); and (iii) we assume that introgressed alleles remain rare such that individuals contain at most one introgressed block. The last assumption is the most critical, as its validity depends on the value of θ. Therefore, we compare our analytical results to forward-in-time individual-based simulations assuming that $Ns \gg 1$ and $cL \ll 1$, but in different introgression regimes by relaxing the assumption (iii).

Simulations were performed with SLiM 3.3 (Haller and Messer, 2019) following a Wright–Fisher life cycle. Two constant-size populations of $N = 100,000$ sexually-reproducing diploid individuals were simulated with discrete and non-overlapping generations. For simplicity, we assume a male-heterogametic sexual system (males are XY, and females are XX) with $1:1$ sex-ratio. We model steady migration from the donor into the recipient species by replacing a fraction m_F of females and a fraction m_M of males by immigrants in each generation. Offspring are then generated by drawing a random mother and a random father according to their fitness (defined below). The offspring's genotype is created from the chosen parents as follows: the first offspring haploid genome is produced via recombination between the two genomes of the female, and the second via recombination between the two genomes of the male (except in the case of sex chromosomes which do not recombine in males). Once all offspring are generated, the offspring generation becomes the new parental generation. Note that unlike the analytical treatment, an individual might contain multiple introgressed fragments.

Simulated genomic blocks, lying either on an autosome or a X chromosome, carry L equally spaced loci, which are fixed for different alleles in the two species at the start of the simulations. Recombination occurs at a uniform rate c_F per locus per generation in females (c_M in males). The expected number of crossovers per generation, within the entire block, is thus $C = c(L-1)$. For each offspring genome, the number of recombination breakpoints is drawn from a Poisson distribution with mean equal to $c(L-1)$ and their positions are chosen by sampling uniformly along the block. We assume null recombination between the X and the Y chromosomes in males. For autosomes, an individual with y loci that carry deleterious alleles in the heterozygous state and y' loci in the homozygous state has relative fitness $v_A(y, y') = e^{-ys_A - y's_{hom,A}}$. For sex chromosomes, the relative fitness of a female is then $v_F(y, y') = e^{-ys_F - y's_{hom,F}}$; while it is $v_M(y) = e^{-ys_M}$ for a male, as it carries a single copy of the X chromosome. Note that the simulation model can be extended to include epistasis by changing the form of the fitness function (as above).

We followed the average frequency of the deleterious alleles in the recipient species across generations, separately for sex chromosomes (i.e. $\overline{p}_X$) and autosomes (i.e. $\overline{p}_A$). Simulations were run for $t = 10,000$ generations, i.e. till much after migration-selection balance was reached. For a given set of parameters, we performed 100 replicate simulations.

We then investigate the effect of the selected block as a barrier against neutral gene-flow. Once migration-selection balance is reached in the recipient species (in practice, after $t = 10,000$ generations), we introduced a neutral marker differentially fixed between them at the extremity of the L-locus block ("rod" configuration). The recombination rate of the neutral marker with the nearest deleterious variant on the selected block is αc. We calculated the effective migration rate of the neutral allele in steady state by monitoring its rate of increase in the recipient species: $m_e = \frac{\overline{u}_{recipient}(t+1) - \overline{u}_{recipient}(t)}{\overline{u}_{donor} - \overline{u}_{recipient}(t)}$, where $\overline{u}_{recipient}(t)$ and $\overline{u}_{donor}$ are the average frequencies of the neutral marker in the recipient and donor species, respectively (see Figure S3A). Note that $\overline{u}_{donor} = 1$, since the donor species is fixed for the neutral allele, and migration

is one-way. In practise, we fitted a linear regression to the log of $\overline{u}_{recipient}(t)$ as a function of the number of generations to estimate its slope (i.e. m_e) using the R function "lm" (from package "stats" v3.6.1, R, 2013); and we calculated its confidence interval using the R function "confint" from the same package. We based our calculation on the first few hundred generations that showed a constant rate of increase of the neutral allele.

Results

Extending previous results (Barton, 1983; Barton and Bengtsson, 1986) to the case of sex chromosomes, we have derived analytical expressions for the equilibrium frequency of multilocus sex-linked incompatibilities, and their strength as barriers against gene exchange between two hybridizing species (eqs. (3) and (5), see also Appendix A and B). We have found that when net selection against introgression is weak ($sL \ll 1$), the sex-linked and autosomal introgression are described by the same deterministic equations, but with different effective parameters: $s_A = \frac{s_F+s_M}{2}$ replaced by $s_X = \frac{s_F+(s_M/2)}{2}$, $m_A = \frac{m_F+m_M}{2}$ replaced by $m_X = \frac{m_F+(m_M/2)}{2}$ and c_A by $c_X = \frac{c_F}{2}$ (see Model and methods).

We now focus on the biological consequences of there being different effective parameters (Table 2 and 3). We summarize the impact of (i) the genetic architecture of the barrier between species, (ii) the existence of dosage compensation and sex-biased forces, and (iii) other model extensions (dominance and epistasis). We restrict attention to the effect of each factor separately, although combined effects are discussed for the interpretation of empirical data (see Discussion).

To be consistent with the mathematical simplifications in our model (see Model and methods), we choose sL to be in the range 0.01 to 0.1, cL to be in the range 0.025 to 0.25 and migration to be weak relative to selection ($m = 0.001$). For the simulations, we assume that the population size is sufficiently large ($N = 10^5$) to conform with a deterministic regime. We typically compare introgression of blocks with the same total selective disadvantage ($S = sL$) and total map length ($C = cL$), but different numbers of barrier loci (L): thus in the figures, the per locus s and c decrease with increasing L. Results are first shown for the basic model (i.e., with co-dominance, multiplicative effects, no dosage compensation and no sex-specific forces), then including sex-specificities, and finally extending the model to dominance and epistasis.

1. Genetic architecture of the barrier between species

Coupling between the barrier loci and migration-to-selection ratio

Validating Barton (1983)'s autosomal results, we found that the steady state frequency of the deleterious alleles decreases as coupling between the selected loci is stronger, i.e., as θ increases (Figure 1A). When coupling between the barrier loci is strong ($\theta_A = 2$, red; Figure 1A), the deleterious block acts as the unit of selection, and so selection maintains a lower steady state frequency of the deleterious alleles in the recipient species ($\overline{p}_A$) than under intermediate coupling ($\theta_A = 1$, black; Figure 1A). When coupling is weak ($\theta_A = 0.2$, blue; Figure 1A), recombination breaks the genomic block down to smaller sub-blocks of weaker selective disadvantage, resulting in a much higher steady state frequency of the introgressing alleles. Note that when $\theta < 1$ and L is large, the analytical solutions break down: $\overline{p}_A$ obtained by simulations (triangles) is much higher than the predicted values (lines and circles). Coupling has a similar effect on the gene flow at a neutral marker, i.e. effective neutral migration decreases as θ increases (and so the barrier strength correspondingly increases; Figure 2), which corroborates Barton and Bengtsson (1986)'s autosomal results.

The $\frac{m}{S}$ ratio determines the expected allele frequency when selected loci are perfectly linked; and it has also a notable impact on the steady state frequency of the deleterious alleles in the recipient species. For example, under a low $\frac{m}{S}$ regime ($\frac{m_X}{S_X} = \frac{m_A}{S_A} = 0.1$, blue; Figure 1B), the autosomal introgression rate is ~ 10 times higher relative to that of a high $\frac{m}{S}$ regime ($\frac{m_X}{S_X} = \frac{m_A}{S_A} = 0.01$, red; Figure 1B).

We show that these patterns hold for the sex chromosomes as well, but with a consistently lower introgression rate and higher barrier strength (Figure 1A and Figure 2). This is because the deleterious alleles on the sex chromosome are more strongly coupled to each other than on the autosomes (i.e., $\theta_X = \frac{3}{2}\theta_A$; Table 3), while the expected deleterious allele frequency is the same for both chromosome types (i.e., $\frac{m_X}{S_X} = \frac{m_A}{S_A}$; Table 3); if we compare an autosome and a sex chromsome with identical genetic architectures (i.e. same s_F, s_M, c_F and L). These relationships result in a lower sex-linked introgression rate when the barrier is multilocus ($\frac{\overline{p}_X}{\overline{p}_A} < 1$ for $L > 1$; Figure 1A), and a higher barrier strength

on the sex chromosome even when there is a single barrier locus ($\frac{b_X}{b_A} > 1$ for $L \geq 1$; Figure 2); since the neutral marker and the selected locus are then more strongly linked.

In scenarios where selection against introgression is very strong ($s_F, s_M \gg c$, i.e. $\theta \gg 1$), the difference between θ_X and θ_A has only a very weak effect on introgression probabilities (red; Figure S4A), while the gap between the two is much more pronounced for lower values of θ (Figure 1A). This simply reflects the fact that introgression rates are much less sensitive to the exact value of the coupling strength, when this is large.

Number of barrier loci lying on the incompatible b*lock*

The influence of the number of barrier loci on the steady state frequency of the introgressing alleles depends on the coupling regime. In a strong coupling regime ($\theta \gg 1$), the steady state introgression rates of sex-linked and autosomal alleles is largely governed by the net selective disadvantage of the block (sL). Therefore, the introgressed allele frequency only increases very weakly with L, and becomes insensitive to L for very large blocks as long as sL remains constant (red; Figure 1A and Figure S4A). At smaller θ values, $\overline{p}_A$ and $\overline{p}_X$ both increase with L (black, Figure 1A); and correspondingly, the strength of the barrier, b_A and b_X, decreases (Figure S3). When coupling is very weak ($\theta \ll 1$), the steady state deleterious allele frequency increases so strongly with L that our predictions break down at large L (blue; Figure 1A). As before, this is beause in the $\theta \ll 1$ regime, loci are only weakly coupled and experience effective selection that is close to the individual selective effect s. The latter decreases as we consider genetic architectures with larger and larger numbers of more weakly selected loci (from left to right on the x-axis in Figure 1).

We also predict that the difference in introgression rate and barrier strength between the two types of chromosome increases with the number of barrier loci involved (L), as long as coupling between selected loci is sufficiently weak (Figure 1A). In this regime, the effective strength of selection against individual loci scales as $L^{2\theta_X}$ and $L^{2\theta_A}$ for X-linked and autosomal deleterious alleles respectively; thus, the ratio of introgression rates scales as $L^{2(\theta_X - \theta_A)}$. Since coupling between X-linked alleles is stronger, this means that in this regime, the ratio of X-linked alleles to autosomal alleles must decrease as the barrier becomes more polygenic. For example, when $\theta_A = 1$ and $\theta_X = 1.5$, introgression on the sex chromosome can be as low as ~ 0.66 that of the autosomes when the incompatible block is polygenic ($L = 100$, black; Figure 1A); while it is identical on both chromosomes when a single barrier locus is acting ($L = 1$). The same qualitative pattern is observed for barrier strength: $\frac{b_X}{b_A} \sim 2$ for $L = 100$ while it is ~ 1.5 for $L = 1$, when the neutral marker is close to the block ($\alpha = 0.01$, black; Figure 2). In contrast, under a strong coupling regime (e.g. $\theta_A = 10$ and $\theta_X = 15$), the differences between the two types of chromosomes becomes negligible (red; Figure S4).

Note that for the barrier strength, only the extreme cases of a single strongly deleterious locus ($L = 1$) and many weakly deleterious loci ($L = 100$) are considered hereafter.

Distance of the neutral marker from the incompatible block

We have modelled a situation in which a neutral marker lies at one end of an incompatible genomic block. On both the autosomes and the sex chromosomes, the barrier strength always decreases as a function of the distance between the neutral marker and the closest selected locus. This is because the ability of a neutral marker to escape from its incompatible genomic background increases with its genetic distance from the selected block. For example, under intermediate coupling (black; Figure 2), a multilocus autosomal barrier can reduce by a factor ~ 20 the effective migration rate of a neutral marker lying at a fraction distance $\alpha = 0.01$ from the closest barrier locus, while this factor drops to less than ~ 2 at a fraction distance $\alpha = 1$; these numbers are respectively ~ 35 and ~ 2.5 in the sex chromosome case.

2. Dosage compensation and sex-biased forces

Dosage compensation

The basic model considered so far does not include dosage compensation, and so the hemizygous selective effect of a deleterious allele in a XY male (or a ZW female) is half as strong as the homozygous effect in a XX female (or a ZZ male). However, various molecular mechanisms of dosage compensation have evolved independently in various clades in

response to these imbalances (Gu and Walters, 2017). In Figure 3A, we tested the effect of full dosage compensation by over-regulation of the sex chromosome in XY males (like in dipterans and hemipterans), so that the effect of a single copy of a sex-linked allele in hemizygous males rises to the level of two copies in homozygous females ($s_M = s_{hom,F} = 2s$ and $s_F = s$ for $h = 0.5$). In such a situation, we have $\theta_X = 2\theta_A$ and $\frac{m_X}{S_X} = \frac{3}{4}\frac{m_A}{S_A}$ (Table 3), which results in a lower X-to-autosome ratio of introgressed allele frequencies for weak to intermediate coupling between selected loci ($\frac{\overline{p}_X}{\overline{p}_A} \sim 0.4$ instead of ~ 0.66 in the basic model with $L = 100$, compare red vs. black; Figure 3A). This holds for single and multilocus barriers (i.e., for $L \geq 1$), since not only coupling between sex-linked alleles is stronger than in the basic model, but also m/S on the sex chromosomes is weaker than on autosomes. Likewise, the influence of dosage compensation on neutral gene flow is to increase the barrier strength relative to the case without compensation ($\frac{b_X}{b_A} \sim 3$ instead of ~ 2 with $L = 100$ and $\alpha = 0.01$, compare red vs. black; Figure 4A).

In Figure S5A, we tested the effect of another mechanism, which compensates the hemizygosity of the sex chromosome by its under-regulation in XX females (like in nematodes; or in ZZ males in lepidopterans). In that case, the effect of a homozygous pair of sex-linked alleles in females is reduced to the level of hemizygous males ($s_{hom,F} = s_M = s_F = s$). To first order in sL and cL, this kind of dosage compensation should have no effect on introgression (i.e., the black and red dotted curves overlap in Figure S5A), since it does not affect heterozygous selective effects, which are the only quantities that matter when introgressed frequencies are low. Instead the general solutions (and simulations) show that the X-to-autosome introgression rate is slightly higher than in the basic model (Figure S5A), and the barrier strength ratio is accordingly weaker (Figure S6A), in agreement with the fact that sex-linked barrier loci in females have weaker deleterious effects under this compensation mechanism. We expect this effect to be enhanced with larger values of S.

Achiasmy

In some species, such as certain dipterans or lepidopterans, recombination is absent throughout the genome in the heterogametic sex (i.e. their meiosis is achiasmate, so $c_M = 0$ on autosomes and sex chromosomes in an XY sexual system). As the sex chromosomes (X or Z) spend one third of their time in the heterogametic sex, while autosomes spend an equal amount of time in both sexes, achiasmy leads to a lower effective recombination rate of autosomes compared to sex chromosomes (all else being equal). In such case, we have $\theta_X = \frac{3}{4}\theta_A$ (Table 3), i.e. the coupling between the barrier loci is stronger along the autosomes than the sex chromosomes. As a consequence, achiasmatic species exhibit higher introgression of sex chromosomes than autosomes when barriers are multilocus (~ 1.2 times higher with $L = 100$, blue; Figure 3A); and their barrier strength is accordingly weaker (~ 0.6 that of autosomes with $L = 100$ and $\alpha = 0.01$, blue; Figure 4A).

Sex-biased migration

Differences in migration rates between sexes are commonly observed in nature, with the heterogametic sex prone to higher migration in mammals and birds (Greenwood, 1980); although there are many exceptions and patterns are less known in other taxa. Sex-biased migration affects only the dynamic of the sex-linked alleles (to lowest order in sL and cL), because the heterogametic and homogametic sexes carry different numbers of sex chromsomes, but the same number of autosomes. Under male-biased migration in a XY system (or female-biased in a ZW system), the migration-to-selection ratio is thus lower for sex-linked alleles than for autosomal alleles (e.g. if $m_M = 3m_F$, then $\frac{m_X}{S_X} = \frac{5}{6}\frac{m_A}{S_A}$; Table 3). Compared to the basic model, this results in a lower X-to-autosome ratio for $L \geq 1$ and weak to intermediate coupling ($\frac{\overline{p}_X}{\overline{p}_A} \sim 0.55$ instead of ~ 0.66 with $L = 100$, red; Figure 3B). Note that barrier strength is predicted to be insensitive to sex-bias in migration to lowest order in sL and cL (see eqs. (4) and (5)). However, for stronger selection, sex-biased migration can have a weak effect on barrier strength, which is predicted by eqs. (22) and (29) (Appendix B), and is also confirmed by our simulations ($\frac{b_X}{b_A} \sim 2.5$ instead of ~ 2 with $L = 100$ and $\alpha = 0.01$, red; Figure 4B). These patterns are reversed relative to the basic model, if migration is female-biased in a XY system (e.g. if $m_F = 3m_M$, then $\frac{m_X}{S_X} = \frac{7}{6}\frac{m_A}{S_A}$; Table 3), or male-biased in a ZW system.

Sex-biased selection

In most species, the strength of sexual selection is stronger in males than in females (Ellegren and Parsch, 2007). Since twice as many females are heterozygous for X-linked introgressed alleles as males (i.e., any X-linked incompatible allele spends twice as much time in females as in males), and that the reverse is true for the Z chromosome, male-biased sexual selection will lead to opposite effects in the two sexual systems. Under a XY system, if selection is e.g. twice as strong on XY males as on females ($s_M = 2s_F$), we have $\theta_X = \frac{4}{3}\theta_A$ and $\frac{m_X}{S_X} = \frac{9}{8}\frac{m_A}{S_A}$ (Table 3), i.e. a weaker coupling and a stronger migration-to-selection ratio on the sex chromosome compared to the basic model. This results in a higher X-to-autosome introgression rate compared to the basic model ($\frac{\bar{p}_X}{\bar{p}_A} \sim 0.9$ instead of ~ 0.66 with $L = 100$, red; Figure 3C), and a correspondingly lower barrier strength ($\frac{b_X}{b_A} \sim 1.5$ instead of ~ 2 with $L = 100$ and $\alpha = 0.01$, red; Figure 4C). On the contrary, when ZZ males are under stronger selection than females ($s_F = 2s_M$, using our XY notation), we have $\theta_Z = \frac{5}{3}\theta_A$ and $\frac{m_Z}{Z} = \frac{9}{10}\frac{m_A}{S_A}$ (Table 3), resulting in lower Z-to-autosome introgression rates compared to the basic model (Figure 3C) and a correspondingly higher barrier strength (Figure 4C).

3. Other model extensions

Dominance of barrier loci

So far, i.e., in Figures 1-4, we have shown results for individual-based simulations in which incompatible mutations have co-dominant effects ($h = 0.5$), and compared these with our analytical predictions (sL and $cL \ll 1$) that are actually independent of dominance as long as selection is weak (see Table 3 and Appendix A). We now examine how dominance affects introgression patterns by considering either partial recessivity ($h = 0.1$) or full dominance ($h = 1.0$) of the incompatible effects, and by changing their homozygous deleterious effect (s_{hom}) while keeping the heterozygous selective effect s constant. That way the influence of $h = s/s_{hom}$ (i.e., the ratio of heterozygous to homozygous effects) can be tested.

Recessivity of deleterious alleles implies that homozygous blocks are far more deleterious than in the co-dominant model ($s_{hom} = 0.5$ for $h = 0.1$ *vs* $s_{hom} = 0.1$ for $h = 0.5$), resulting in a strong selective disadvantage for first generation immigrants (who carry two copies of the block). This leads to lower levels of introgression for both the sex chromosome and autosomes in the simulations (blue; Figure S5B). Moreover, X-linked alleles cannot be found in homozygous state in the heterogametic sex, and so they cause less deleterious effects than in females (where they are homozygous in migrants and in rare recombinant individuals); while autosomal alleles are as deleterious in both sexes. This difference explains why in simulations the X-to-autosome introgression ratio is higher than that in the co-dominant case (Figure S5B), and the barrier strength ratio is correspondingly smaller (Figure S6B). However, it is worth noting that introgression remains low overall in our model, and so homozygous blocks are rare in the population. They are actually neglected in the first order analytical predictions (lines) and they only appear in non-hemizygous migrants in the more general predictions (filled symbols); but they are fully considered in the simulations (empty symbols). Therefore, the influence of dominance (h) on introgression rates and barrier strengths is by itself small: what matters to first order is only the heterozygous effects (s) of the incompatible alleles.

If we also assume dosage compensation by up-regulation of the X in males, then the migration-to-selection ratio ($\frac{m}{S}$) of X-linked recessive alleles is only $\frac{1}{4}$ that of the autosomes (compared to $\frac{3}{4}$ when alleles are co-dominant, see Table 3); and coupling between incompatible alleles (θ) is 6 times stronger on the X chromosome relative to autosomes (compared to 2 times when alleles are co-dominant, see Table 3). Importantly, these two effects cause a much lower X-to-autosome introgression ratio than under co-dominance ($\frac{\bar{p}_X}{\bar{p}_A} \sim 0.1$ instead of ~ 0.4 with $L = 100$, blue; Figure S5C), and also a much greater X-to-autosome difference in barrier strength ($\frac{b_X}{b_A} \sim 20$ instead of ~ 3.5 with $L = 100$ and $\alpha = 0.01$, blue; Figure S6C). This parameter setting is important to consider as it leads to very different heterozygous X-linked effects in males and females, which is at the basis of the dominance theory (Turelli and Orr, 1995, 2000).

If we assume complete dominance of the incompatible alleles, then homozygous blocks are just as deleterious as heterozygous blocks ($s_{hom} = 0.05$ for $h = 1.0$), and this leads to sligthly higher levels of introgression for both chromosome types in the simulations (red; Figure S5B), compared to the co-dominant model. With dosage compensation, the relation-

ship between the effective parameters becomes $\theta_X = \frac{3}{2}\theta_A$ and $\frac{m_X}{S_X} = \frac{m_A}{S_A}$ (Table 3); therefore dominant X-linked alleles introgress more than co-dominant alleles (red; Figure S5C), and act as weaker barrier to gene flow (red; Figure S6C).

Epistasis among barrier loci

We have assumed so far that selection acts independently (i.e., multiplicatively) against incompatible introgressing alleles. However, deleterious interaction between them (i.e. negative epistasis, $\varepsilon < 1$) is an important component of speciation and is the basis of the seminal DMI model (Dobzhansky, 1937; Muller, 1940). Therefore, we now evaluate a version of the model where all loci act epistatically ($\beta = 1$), and the fitness of an incompatible block decreases non-linearly with the number of barrier loci it carries (note that this is a quite different version of epistasis than in the DMI model, see Model and methods). Epistasis acts by strongly decreasing the introgression rate of both autosomes and sex chromosomes as a function of their number of incompatible loci (when $L \geq 1$, blue and red; Figure S5D). Accordingly, the strength of an epistatic multilocus barrier is much stronger than in the multiplicative case (by a factor $\sim 10^4$ with $L = 100$, $\alpha = 0.01$ and $\varepsilon = 0.1$; Figure S6D). Importantly, and contrary to the multiplicative model, there is a deficit of autosomal to sex-linked introgression when the number of deleterious loci is sufficiently large (say $L \gg 10$), which amplifies with the number of incompatible alleles (blue and red; Figure S5D). The difference in introgression rate between the two chromosome types can be as large as $\frac{\overline{p}_X}{\overline{p}_A} \sim 12$ (with $L = 100$ and $\varepsilon = 0.1$, red; Figure S5D), which leads to an autosomal barrier strength ~ 30 times higher than that of the sex chromosome (with $L = 100$, $\alpha = 0.01$ and $\varepsilon = 0.1$, red; Figure S6D). This happens because with epistasis, the decreased fitness of immigrants and F1 hybrids, which carry entire incompatible blocks, prevails over that of later generation hybrids (which carry shorter incompatible blocks); and considering that immigrant alleles are selected against more heavily on autosomes relative to sex chromosomes due to the hemizygous selection acting on migrant XY males (in the absence of dosage compensation).

Table 3. Evolutionary scenarios

The predicted values of θ and $\frac{m}{S}$ are derived fron the analytical solution in eq. (3) (which assumes sL and $cL \ll 1$), and so they are independent of the dominance coefficient (h). See Table 1 for the significance of model parameters. Note that under dominance ($h = 1.0$), the two dosage compensation mechanisms are identical to the basic model with dominance.

Scenarios		Parameters		Predicted	
		autosome	**X**	**coupling, θ**	$\frac{m}{S}$
Basic model		$\beta = 0$ $h = 0.5$ $c_F = c_M = c$ $m_F = m_M = m$ $s_F = s_M = s$ $s_{hom,F} = s_{hom,M} = \frac{s}{h} = 2s$	$\beta = 0$ $h = 0.5$ $c_F = c$; $c_M = 0$ $m_F = m_M = m$ $s_F = s_M = s$ $s_{hom,F} = \frac{s}{h} = 2s$	$\theta_X = \frac{3}{2}\theta_A$	$\frac{m_X}{S_X} = \frac{m_A}{S_A}$
	for $h = 1.0$ for $h = 0.1$	$s_{hom,F} = s_{hom,M} = s$ $s_{hom,F} = s_{hom,M} = 10s$	$s_F = s_M = s_{hom,F} = s$ $s_{hom,F} = 10s$	as basic model	as basic model
Dosage compensation (X up-regulation in ♂)	 for $h = 0.5$ for $h = 0.1$	 as basic model $s_{hom,F} = s_{hom,M} = 10s$	$s_F = s$; $s_M = s_{hom,F} = \frac{s}{h}$ $s_F = s$; $s_M = s_{hom,F} = 2s$ $s_F = s$; $s_M = s_{hom,F} = 10s$	$\theta_X = (1 + \frac{1}{2h})\theta_A$ $\theta_X = 2\theta_A$ $\theta_X = 6\theta_A$	$\frac{m_X}{S_X} = (\frac{3}{2+1/h})\frac{m_A}{S_A}$ $\frac{m_X}{S_X} = \frac{3}{4}\frac{m_A}{S_A}$ $\frac{m_X}{S_X} = \frac{1}{4}\frac{m_A}{S_A}$
Dosage compensation (X down-regulation in ♀)	for $h = 0.5$ for $h = 0.1$	as basic model $s_{hom,F} = s_{hom,M} = 10s$	$s_F = s_M = s_{hom,F} = s$	as basic model	as basic model
Achiasmy		$c_M = 0$	as basic model	$\theta_X = \frac{3}{4}\theta_A$	as basic model
Sex-biased migration	 for $k = 3$ (♀-biased) for $k = 1/3$ (♂-biased)	$m_F = km_M = m$ $m_F = 3m_M = m$ $m_F = \frac{m_M}{3} = m$	$m_F = km_M = m$ $m_F = 3m_M = m$ $m_F = \frac{m_M}{3} = m$	as basic model	$\frac{m_X}{S_X} = \frac{(2+4k)}{(3+3k)}\frac{m_A}{S_A}$ $\frac{m_X}{S_X} = \frac{7}{6}\frac{m_A}{S_A}$ $\frac{m_X}{S_X} = \frac{5}{6}\frac{m_A}{S_A}$
Sex-biased selection	 for $k = 2$ (♀-biased) for $k = 1/2$ (♂-biased)	$s_F = ks_M = s$ $s_F = 2s_M = s$ $s_F = \frac{s_M}{2} = s$	$s_F = ks_M = s$ $s_F = 2s_M = s$ $s_F = \frac{s_M}{2} = s$	$\theta_X = \frac{(2k+1)}{(k+1)}\theta_A$ $\theta_X = \frac{5}{3}\theta_A$ $\theta_X = \frac{4}{3}\theta_A$	$\frac{m_X}{S_X} = \frac{(3+3k)}{(2+4k)}\frac{m_A}{S_A}$ $\frac{m_X}{S_X} = \frac{9}{10}\frac{m_A}{S_A}$ $\frac{m_X}{S_X} = \frac{9}{8}\frac{m_A}{S_A}$

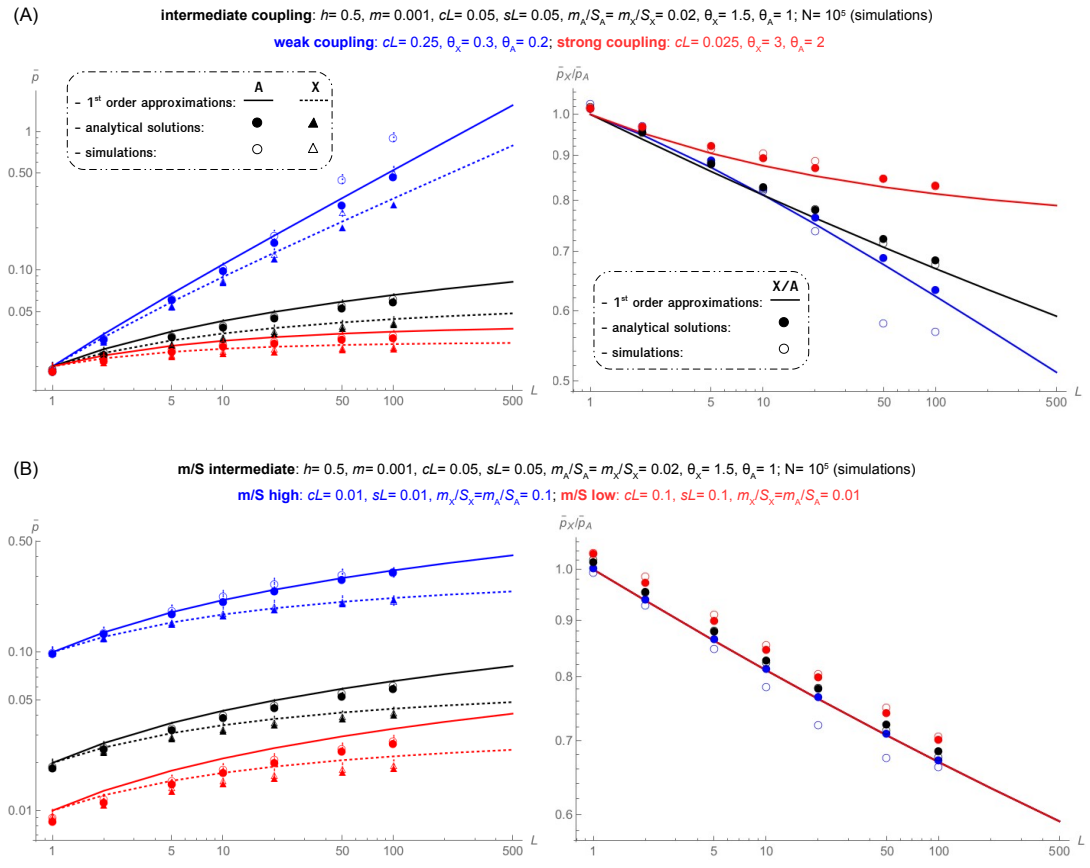

Figure 1. Effect of θ and $\frac{m}{S}$ on average introgression rates

Left panels: Average frequency of the deleterious alleles in the recipient species (autosomal: $\overline{p}_A$; X-linked: $\overline{p}_X$) plotted against the number of selected loci lying on the genomic block, L. The effect of two composite parameters governing introgression is shown: **(A)** $\frac{m}{S}$ determines the expected allele frequency when selected loci are perfectly linked; **(B)** $\theta = \frac{s}{c}$ determines the extent of coupling between loci. Without sex specificity or differences between autosomes and X chromosomes, we have $\theta_X = \frac{3}{2}\theta_A$ and $\frac{m_X}{S_X} = \frac{m_A}{S_A}$, so the deleterious alleles on the X are more strongly coupled to each other than on autosomes, resulting in lower introgression rates ($\frac{\overline{p}_X}{\overline{p}_A} < 1$) when $L > 1$ (right panel). This dependence on L is stronger for smaller values of θ. Lines show the analytical expression in eqs. (11) (Appendix A) and (3) (which are given in terms of composite parameters and are valid for sL, cL and $m \ll 1$); filled symbols show analytical expression in eqs. (10) and (15) in Appendix A (which are also valid for strong selection); empty symbols show results of individual-based simulations iterated for 10,000 generations and averaged over 100 replicates (error bars indicate the standard error of the mean). Colors stand for values of the composite parameters, θ and $\frac{m}{S}$. In the left panels, autosomes are depicted with solid lines, ● and ○, while X chromosomes with dotted lines, ▲ and △. In the right panels, the $\frac{\overline{p}_X}{\overline{p}_A}$ ratio is shown with solid lines, ● and ○. Note that the total selective effect of the block (sL) and its total recombination rate (cL) are kept constant as we vary the number of loci (L; x axis) such that the selective effect per locus (s) and the recombination rate per locus (c) both decrease with increasing L.

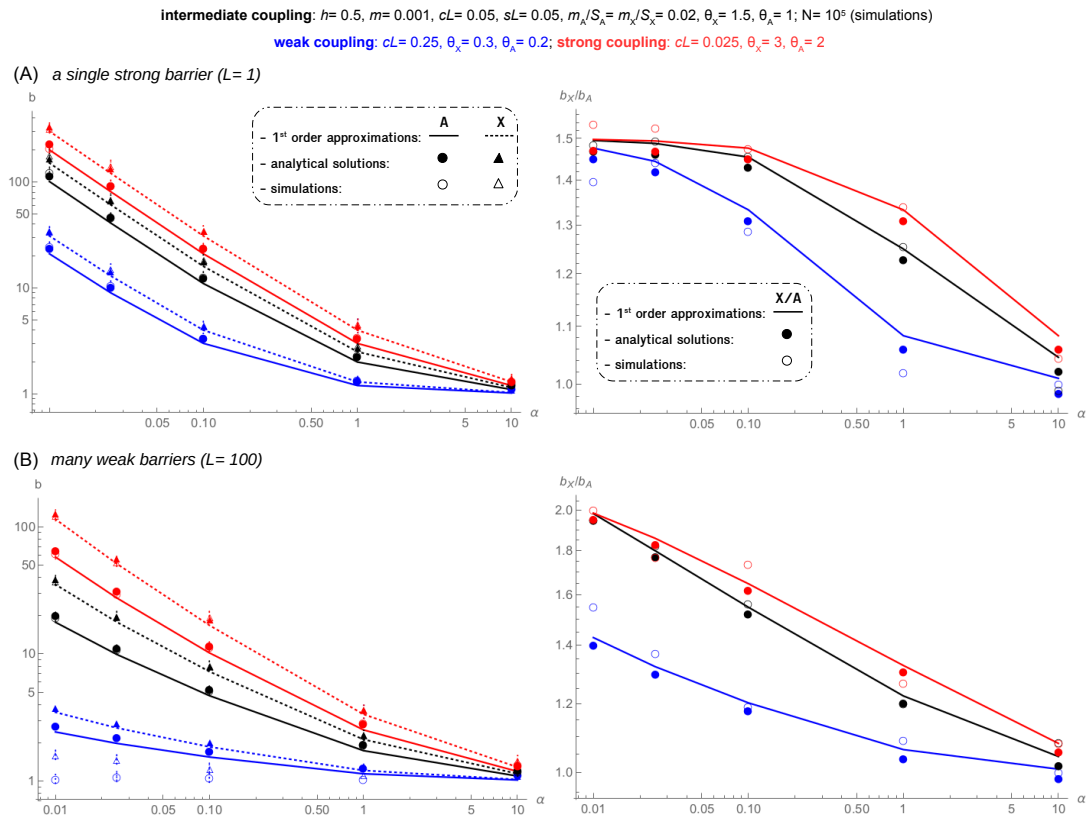

Figure 2. Effect of θ on barrier strength at the neutral marker

Barrier strength at the neutral marker (autosomal: b_A; X-linked: b_X) plotted against its proximity to the nearest selected locus, α. In **(A)** the neutral marker is linked to a single selected locus ($L = 1$); while in **(B)** it is linked to one hundred selected loci ($L = 100$). Lines show the analytical expression in eqs. (4) and (5) (which are given in terms of composite parameters and are valid for sL, cL and $m \ll 1$); filled symbols show analytical expression in eqs. (22) and (29) in Appendix B (which are also valid for strong selection); empty symbols show results of individual-based simulations iterated for 10,000 generations after equilibrating at the selected loci and averaged over 100 replicates (error bars indicate the confidence interval of the estimate). Colors stand for values of the composite parameter $\theta = \frac{s}{c}$ at the selected loci. In the left panels, autosomes are depicted with solid lines, ● and ○, while X chromosomes with dotted lines, ▲ and △. In the right panels, the $\frac{b_X}{b_A}$ ratio is shown with solid lines, ● and ○. Note that the total selective effect of the block (sL) and its total recombination rate (cL) are kept constant across the number of loci (L). Note that the recombination rate between the neutral marker and the nearest selected locus is αLc, therefore lower α values means closer proximity.

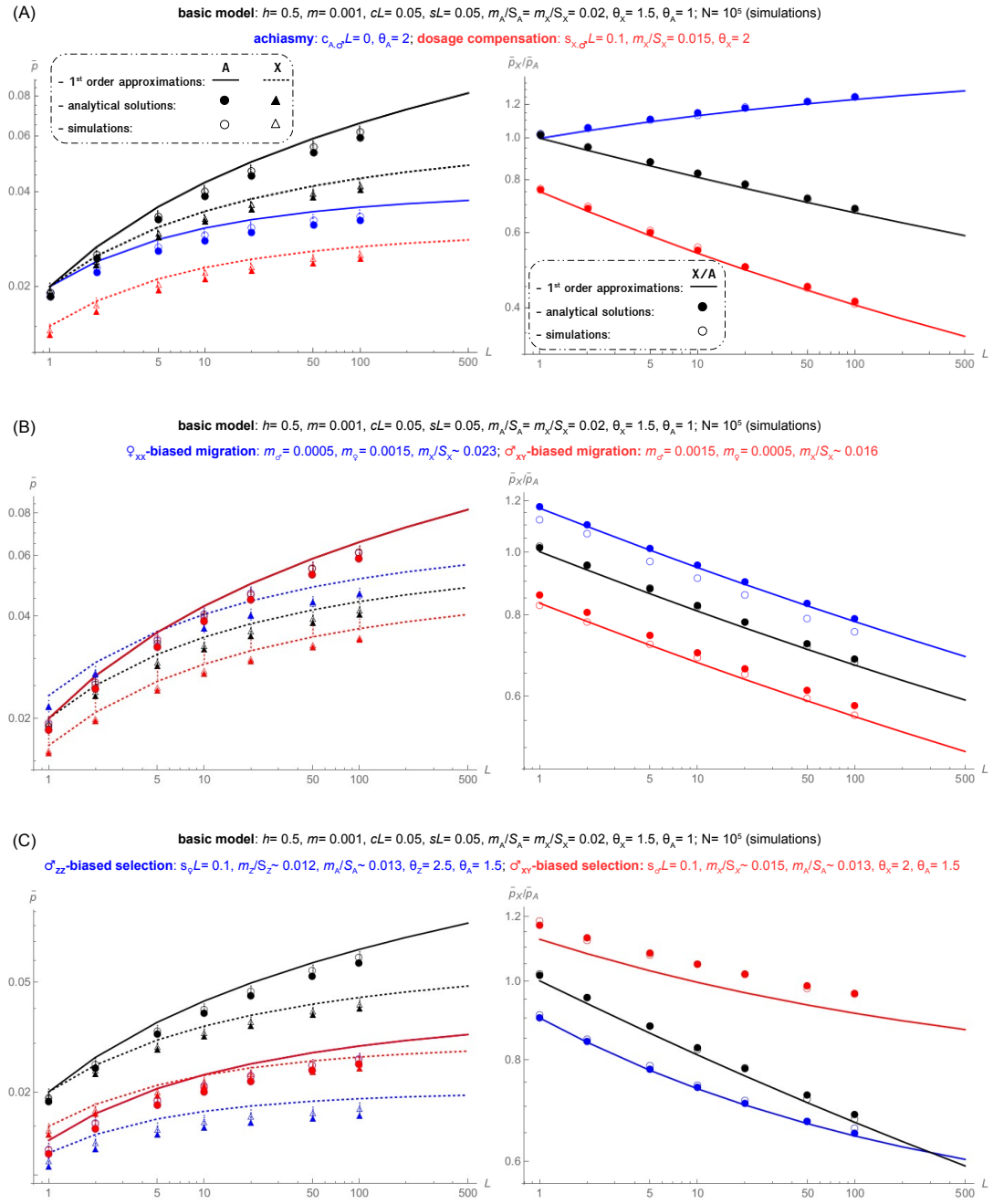

Figure 3. Effect of sex-specificities on average introgression rates

Average frequency of the deleterious alleles in the recipient species (autosomal: $\overline{p}_A$; X-linked: $\overline{p}_X$) plotted against the number of selected loci lying on the genomic block, L. **(A)** Dosage compensation by up-regulation of the X in males ($s_M = s_{hom,F} = 2s$ and $s_F = 2s$ for sex-linked alleles, red) and achiasmy in XY males ($c_M = 0$, blue). **(B)** Sex-biased migration: e.g., if males migrate three times more than females ($m_M = 3m_F$, red); or females migrate three times more than males ($m_F = 3m_M$, blue). **(C)** Sex-biased selection: e.g. if selection is twice as strong on XY males as on females ($s_M = 2s_F$, red); or selection is twice as strong on ZZ males as on females ($s_F = 2s_M$, blue). The basic model is shown in black in all panels. Other details match Figure 1.

(A) **basic model**: h= 0.5, m= 0.001, cL= 0.05, sL= 0.05, m_A/S_A= m_X/S_X= 0.02, θ_X= 1.5, θ_A= 1; N= 10^5 (simulations)

achiasmy: $c_{A,♂}L$= 0, θ_A= 2; **dosage compensation**: $s_{X,♂}L$= 0.1, m_X/S_X= 0.015, θ_X= 2

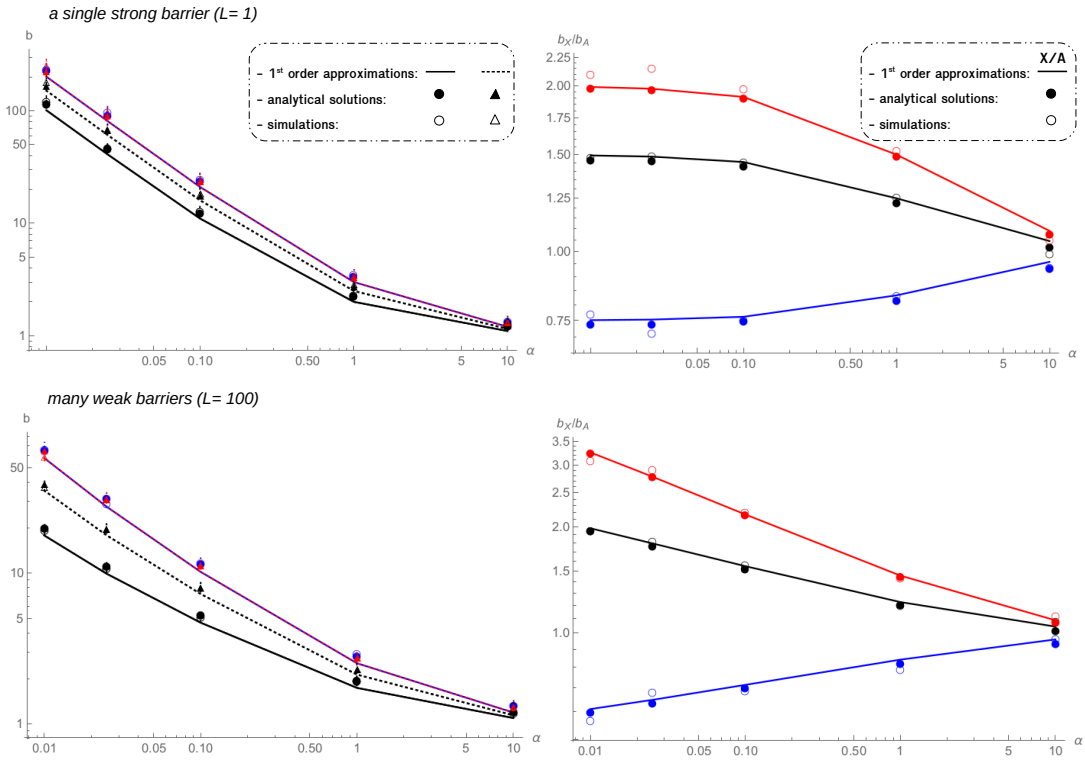

(B) **basic model**: h= 0.5, m= 0.001, cL= 0.05, sL= 0.05, m_A/S_A= m_X/S_X= 0.02, θ_X= 1.5, θ_A= 1; N= 10^5 (simulations)

♀$_{XX}$-biased migration: $m_♂$= 0.0005, $m_♀$= 0.0015, m_X/S_X~ 0.023; **♂$_{XY}$-biased migration:** $m_♂$= 0.0015, $m_♀$= 0.0005, m_X/S_X~ 0.016

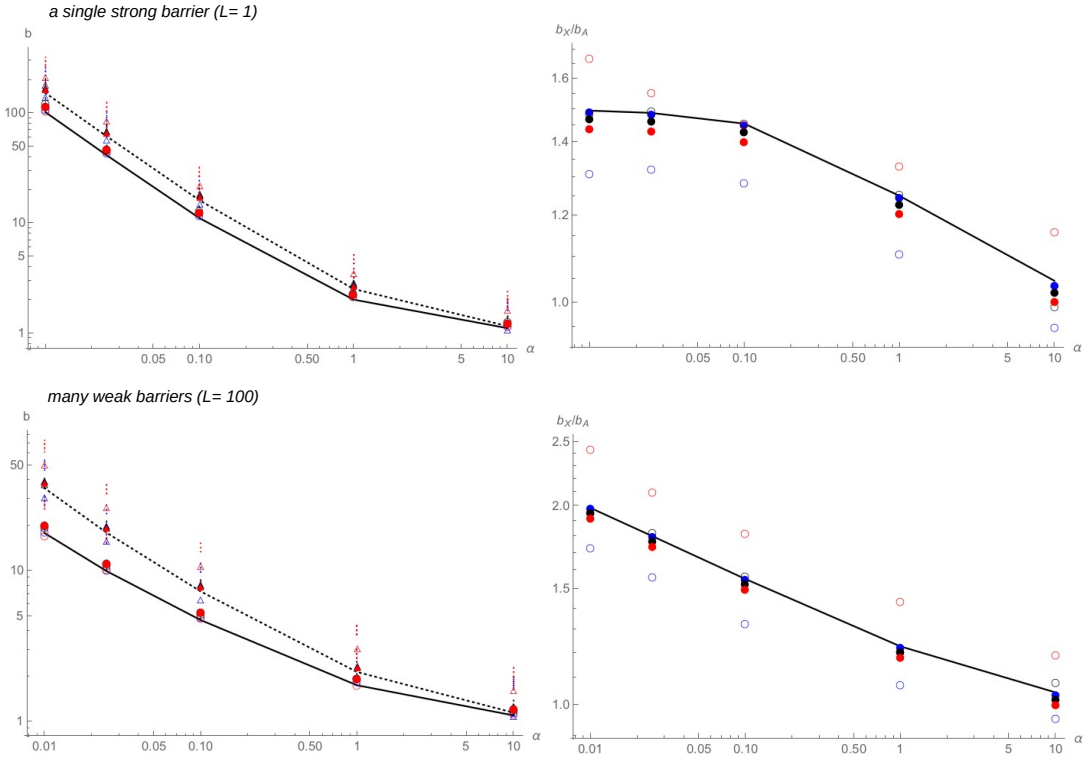

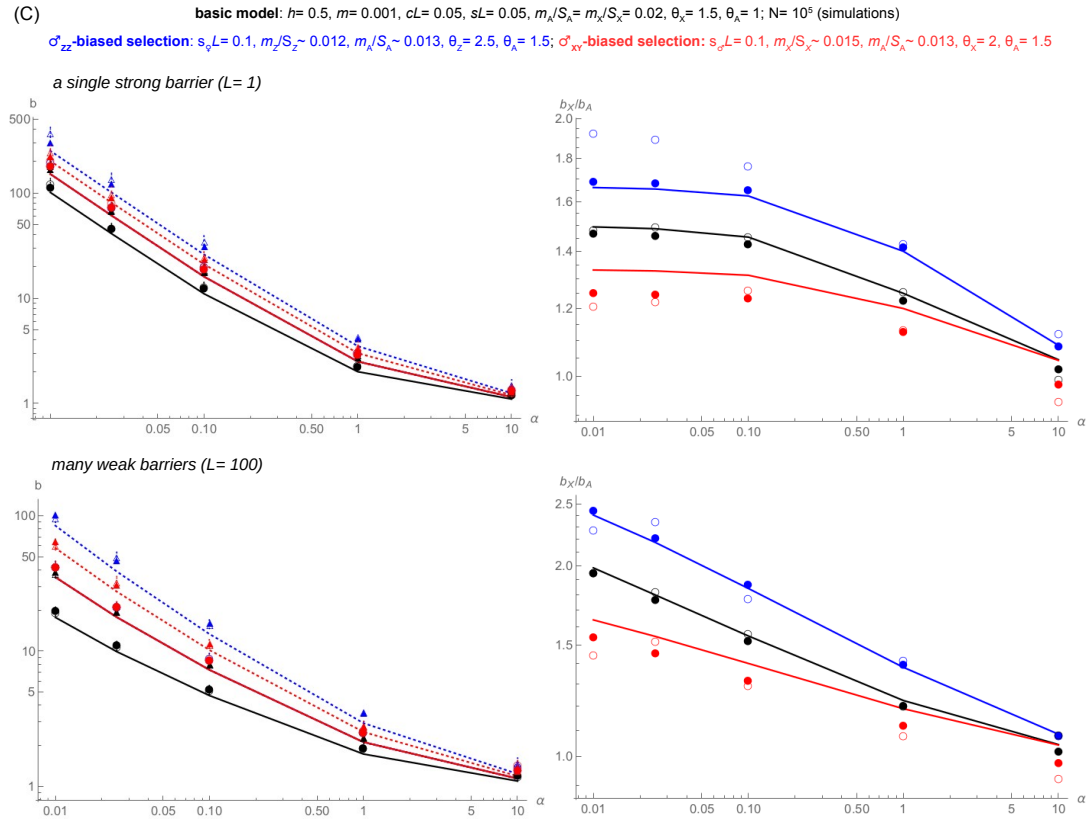

Figure 4. Effect of sex-specificities on barrier strength at the neutral marker

Barrier strength at the neutral marker (autosomal: b_A; X-linked: b_X) plotted against its proximity to the nearest selected locus, α. **(A)** Dosage compensation by up-regulation of the X in males ($s_M = s_{hom,F} = 2s$ and $s_F = 2s$ for sex-linked alleles, red) and achiasmy in XY males ($c_M = 0$, blue). **(B)** Sex-biased migration: e.g., if males migrate three times more than females ($m_M = 3m_F$, red); or females migrate three times more than males ($m_F = 3m_M$, blue). **(C)** Sex-biased selection: e.g. if selection is twice as strong on XY males as on females ($s_M = 2s_F$, red); or selection is twice as strong on ZZ males as on females ($s_F = 2s_M$, blue). The basic model is shown in black in all panels. Other details match Figure 2.

Discussion

Previous work has studied the effect of divergence at large numbers of autosomal loci on genetic exchange between hybridizing species (Barton, 1983; Barton and Bengtsson, 1986). Here, we have extended the analysis to the effects of sex chromosomes. Predictions for the introgression of multilocus deleterious blocks (eq. 3), and their strength as barriers to neutral gene flow (eq. 5), are governed by the same equations as for autosomes, (eqs. 11 and 4) conditional upon a change in the effective parameters. Even though a typical male and female are both heterozygous for X-linked alleles under our model assumptions: (i) males still contribute half as much as females to migration (i.e., $m_X = \frac{m_F+(m_M/2)}{2}$), because female migrants carry two copies of the sex chromosome while males only one; (ii) the same is true for selection (i.e.,$s_X = \frac{s_F+(s_M/2)}{2}$), because half as many males are heterozygous for any introgressed blocks as females; and (iii) males do not contribute at all to recombination (i.e., $c_X = \frac{c_F}{2}$), because they are hemizygous for the sex chromosome. This implies that evolutionary forces differently affecting males and females can be readily encapsulated by these effective parameters, and their biological consequences predicted.

Below, we first summarize the conditions under which sex chromosomes are expected to play a stronger role than autosomes in the maintenance of reproductive isolation in parapatry; then, we confront our theoretical predictions with empirical data from various sexual systems (Table 4); and finally we discuss several limitations of the model.

1. Conditions for an outsized role of sex chromosomes in speciation

Almost one hundred years ago (Haldane, 1922; Dobzhansky, 1936), interspecies crossing experiments laid the foundation for the "two rules of speciation", which imply a major role of sex chromosomes in speciation. Although these rules generally hold across many different species (especially Haldane's rule; Schilthuizen et al., 2011), there has been substantial debate in the literature about their causes. In this study, we shed light on the factors influencing the capacity of sex chromosomes and autosomes to keep species apart in parapatry.

We find that the increased coupling of incompatible alleles on the sex chromosome reduces the escape probability of neutral markers, and so enhances their barrier strength by a factor of ~ 1.5 to ~ 3 relative to autosomes under optimal conditions (i.e. when the neutral marker is close to a multilocus barrier). This result mirrors earlier predictions for single and two-locus barriers under a regime where introgressed alleles are rare (Muirhead and Presgraves, 2016); and for the maintenance of DMIs in parapatry (Hoellinger and Hermisson, 2017). Albeit it is a moderate effect, this process is very general as it applies to species diverging in parapatry under various scenarios (including dosage compensation, sex-biased migration and sex-biased selection). For that reason, it is an appealing explanation for the "two rules of speciation".

Moreover, the greatest sex chromosome-to-autosome difference in barrier strength ($\frac{b_X}{b_A} \sim 20$) occurs when incompatible alleles are recessive and dosage compensated in the heterogametic sex (in agreement with Muirhead and Presgraves (2016); and Hoellinger and Hermisson (2017) who assume recessivity of the DMI itself). Importantly under our model assumptions, dominance (i.e. the ratio of heterozygous to homozygous fitness) has itself little effect as it affects only the selective disadvantage of migrants in the first generation (and of rare homozygous individuals in the simulations). This pattern has also be found by Hoellinger and Hermisson (2017), but it has not been tested in Muirhead and Presgraves (2016). What is happening under recessivity and dosage compensation is that, effectively, the heterozygous deleterious effects of X-linked alleles are much stronger in males than in females. This is at the basis of the dominance theory (Turelli and Orr, 1995, 2000), which proposes that if most incompatible alleles act recessively in hybrids, then their deleterious effects would be more exposed on the sex chromosomes (as they are hemizygous in males). Therefore, selection removes more efficiently recessive incompatible alleles from the sex chromosome. It requires that most deleterious alleles are heterozygous in the recipient species (i.e. during the first hybrid generations), and that the most deleterious allelic effects are due to hemizygous X-linked alleles in males. To date, the dominance theory has been experimentally shown almost exclusively in Drosophila (e.g. Cattani and Presgraves (2012) and Llopart et al. (2018); but see Matsubara et al. (2015) for a study in rice).

Another striking result is that polygenic barriers comprised of many weakly coupled alleles exhibit a greater sex chromosome-to-autosome difference than strong single-locus barriers (although the absolute strength of the barrier is stronger on the latter case). Therefore, the genetic architecture of reproductive isolation affects the extent of introgression on sex chromsomes relative to autosomes, and this may have important implications. QTL mapping studies for sterility and/or inviability of hybrids typically detect a few large-effect loci (Maheshwari and Barbash, 2011), but numerous smaller-effect incompatibilities may be commonly underestimated in these studies. Detailed back-crossing experiments have actually shown that each introgressed block might contain multiple linked barrier loci each required for reproductive isolation to appear (for a review see Fraïsse et al., 2014).

Finally, we predict that the degree of difference between sex chromosomes and autosomes in their ability to maintain species barriers should vary among taxa with different dosage compensation mechanisms (Gu and Walters, 2017) or sex-bias regimes (Hedrick, 2007); although changes may be too subtle to be observed in real data (see below). If the level of expression of a mutation reflects the intensity of its selective effects, then the absence of full dosage compensation (as in female birds; Ellegren et al., 2007) would diminish the magnitude of the deleterious sex-linked effects in the heterogametic hybrids.

We have shown that mechanisms over-regulating the sex chromosome in XY males (e.g., its expression is doubled in dipterans) reinforce the barrier strength of sex chromosomes relative to autosomes by a factor ~ 1.5 compared to species without dosage compensation (in line with Hoellinger and Hermisson, 2017). This is because a single X-linked incompatible allele in males acts as strongly as two X-linked alleles in females. In contrast, the under-regulation of the sex chromosomes in XX females (e.g., nematodes) or in ZZ males (e.g., lepidopterans) slightly decreases the relative barrier strength from $\frac{b_X}{b_A} \sim 2$ (in the absence of dosage compensation) to $\frac{b_X}{b_A} \sim 1.75$. In mammalian females, one of the two X chromosomes is randomly inactivated, and so they are functionally hemizygous, but at the cell level. Therefore, it is unclear how this hemizygosity translates into the individual level, except for marsupials where the paternal X inactivation makes females phenotypically hemizygous, like males (Deakin et al., 2009). Although we did not implement this model, we can expect that this mechanism would accentuate the barrier strength of the sex chromosomes, since sex-linked incompatibilities would then be unmasked in both sexes.

Significant differences in the genetic parameters governing introgression and barrier strength (i.e., m, s and c) exist between the sexes (Hedrick, 2007). First, a general trend is that migration is biased towards the heterogametic sex (males in mammals and females in birds; Greenwood, 1980). As the heterogametic sex carries only one copy of the sex chromosome vs. two for each autosome, this type of sex-bias leads to a deficit of the number of migrating X (or Z) relative to autosomes. Accordingly, we observed that both male-biased migration (in XY systems) and female-biased migration (in ZW systems) boost the barrier strength of the sex chromosomes. As a consequence, we do not expect systematic differences between the two sexual systems. But again, effects are weak: we only observed a ~ 1.25-fold increase in barrier strength assuming that males migrate three times more than females, and that selection is rather strong (see Hoellinger and Hermisson, 2017 for similar patterns). Moreover, when selection is weaker, barrier strength is predicted to be independent of sex-biased migration.

Second, there is a tendency for sexual selection to be stronger in males relative to females (Ellegren and Parsch, 2007). If sexual selection contributes to reproductive isolation between incipient species, then the impact of male-biased sexual selection should vary between XY systems (where males are heterogametic and the X spends $\frac{1}{3}$ of its time) and ZW systems (where males are homogametic and the Z spends $\frac{2}{3}$ of its time). Assuming a two-fold selection bias toward males, we show that the barrier strength of the Z relative to autosomes is increased by a factor ~ 1.5; while for the X, it is decreased by a factor ~ 1.25.

Third, quantitative differences in recombination rate between sexes are common (heterochiasmy; Lenormand and Dutheil, 2005); and even in some cases, recombination is totally absent in the heterogametic sex (26 cases of achiasmy reported; Satomura et al., 2019). As the sex chromosomes spend less time in the heterogametic sex ($\frac{1}{3}$ of its time in XY males or in ZW females) than autosomes do ($\frac{1}{2}$ of their time), achiasmy enhances the opportunity for neutral alleles to

escape from the sex-linked incompatible loci to the extent that the sex chromosomes become a weaker interspecies barrier than autosomes ($\frac{b_X}{b_A} \sim 0.6$; confirming the trend of Muirhead and Presgraves, 2016). Again, this effect is small, and it should not produce systematic differences between the X and the Z chromosomes.

It is worth noting that the above predictions are expected to hold true only for "classic" sex chromosomes, i.e. when the degeneracy of the Y (or W) leaves the X (or Z) hemizygous and non-recombining in the heterogametic sex (Vicoso, 2019). However, in many taxa (e.g. in most reptiles, fish and amphibians; Bachtrog et al., 2014), the length and gene content of the two sex chromosomes are similar (a.k.a. homomorphic sex chromosomes). As a result, both copies remain functional in both sexes, and they recombine along most of their length. Therefore, in absence of sex-biased forces, homomorphic sex chromosomes should behave like autosomes in our model.

2. Insights from empirical data

A direct test of the above theoretical predictions is based on the estimation of the level of reproductive isolation between pairs of species from experimental crosses. This method is therefore only feasible in a limited number of species that can be maintained in the laboratory and cross-bred. For example, Lima (2014) showed that reproductive isolation evolves faster between animal and plant species carrying heteromorphic sex chromosomes, slower in those with homomorphic sex chromosomes, and the slowest between species without sex chromosomes. Although this meta-analysis is indicative of an outsized role for "classic" sex chromosomes in speciation, it is limited by the fact that isolation is being evaluated in laboratory experiments on first generation hybrids only. The barrier effect to interspecific gene flow is therefore not tested under long-term natural conditions.

Next-generation data from a diversity of organisms has provided alternative methods to scan genomes for interspecies reproductive barriers, and contrast autosomes with sex chromosomes. Providing that speciation takes place in the presence of gene flow, we expect that incompatibilities and their surrounding loci would be characterized by a lower rate of interspecific introgression than the rest of the genome (Roux et al., 2013; Sethuraman et al., 2019). This mode of speciation may well be common, since the periodicity of ice ages causes episodes of population contraction/expansion, associated with periods of isolation in refugia, and contact phases during which gene flow is again made possible (Hewitt, 2000). In contrast, if speciation occurs in allopatry, it becomes impossible to locate the barrier loci, because interspecies divergence is then a simple function of the time elapsed since isolation, which is shared by the whole genome (Wilkinson-Herbots, 2008).

By putting together population genomics studies of speciation, Presgraves (2018)'s meta-analysis provides useful insights for the role of sex chromosomes in speciation. He shows that sex chromosomes have a systematically higher differentiation level relative to autosomes in 101 species pairs for which F_{ST} was reported. However, as acknowledged by the author, the impact of confounding factors occurring within species (like demographic events or linked selection) are hard to tell apart from the effect of refractory gene flow on genomic divergence; especially when summary statistics are applied.

To address this issue, we report on Table 4 empirical studies that statistically evaluate speciation models from genomic data (at the two extremes: a model of allopatric speciation vs a model where speciation is opposed by continuous gene flow; Sousa and Hey, 2013), and then test whether sex chromosomes are more resistant to interspecies introgression than autosomes by estimating the introgression rate for each chromosome type. Since cline analyses also provide unambiguous estimates of barrier strength (Barton and Hewitt, 1985), and simulations studies have shown that incompatible sex-linked alleles flow more slowly than autosomal alleles across a cline (Wang, 2013; Hvala et al., 2018; Sciuchetti et al., 2018), we also include them in the table; together with studies inferring introgressed tracts from phased genomes (Lawson et al., 2012).

Redundant studies were eliminated to only include the newer studies with larger sample size in terms of individuals and genetic markers. We investigate a wide range of species (34 species pairs, including 16 XY systems and 18 ZW systems)

characterized by diverse mechanisms of dosage compensation and sex-biased forces (Table 4). Sex chromosomes (X or Z) are old and heteromorphic, except in amphibians and plants. Studies are a mixture of genome-scale data and old school multilocus surveys, including six studies with five or less loci available for sex chromosomes and/or autosomes. Note that given the small number of studies for each factor combination (in terms of sex chromosome features and sex bias; Table 4), we preclude to draw any quantitative conclusions.

Overall, patterns are mixed with $\sim 52\%$ of the studies showing lower migration rates, steeper clines and/or lower fraction of introgressed tracts on the sex chromosomes compared to the autosomes ($\frac{8}{16}$ in XY studies and $\frac{10}{18}$ in ZW studies). This apparent inconclusive result hides a strong heterogeneity between clades.

In XY systems with old sex chromosomes, almost all mammalian species exhibit stronger X-linked barriers relative to autosomes, in agreement with their type of dosage compensation (X chromosome inactivation) and with the prevalence of male-biased migration, but not with sexual selection being predominantly male-biased. On the contrary, none of the studies in *Drosophila* (except one) shows that the X chromosome is less exchangeable between species than autosomes. This is in line with the fact that the species studied are achiasmatic, although this effect could be counter-balanced by their mechanism of dosage compensation (X up-regulation in males). Moreover, the sampling of other genera would be required to draw more general conclusions in dipterans. The other two XY clades possess young sex chromosomes. Amphibians carry homomorphic sex chromosomes, but they display ambiguous results (one study complies with the predictions and the other not). The only survey in plants demonstrates that the young X chromosome has an outsized role in speciation, and this may be due to their mechanism of dosage compensation (Filatov, 2018).

In ZW systems, the only survey in Lepidoptera reveals that the Z is a stronger barrier to gene flow than autosomes, which is in contradiction with its mode of dosage compensation (under-regulation of the Z in females) and with the prevalence of achiasmatic species (but note that the studied species was not tested for achiasmy). Finally, birds present a balanced mixture of the two patterns across the six orders examined. On one side, both the prevalence of female-biased migration and male-biased sexual selection in birds should boost the strength of the Z-linked barriers; but on the other side, their absence of full dosage compensation may counteract this effect.

Although indicative on the validity of our theoretical predictions, these conclusions should be considered preliminary. The first caveat concerns the taxonomic sampling, which is overweighted by some clades (e.g. bird species) or some genus within clades (e.g. *Drosophila*), and likely influenced by positive results; altogether these factors may introduce systematic biases in the global picture. Second, information concerning the mechanisms of dosage compensation or the existence of sex bias are generally reported at the level of the order instead of the species; and so this precludes a definite test of their impact. Moreover, the balance of power among the sex-biased evolutionary forces will depend on their respective magnitude, which is very hard to measure in nature.

Also, there may be systematic differences between the statistical methods in their ability to detect differences between the two types of chromosomes. For example, all ($\frac{3}{3}$) haplotype-based studies show a major role of the sex chromosome, while only $\frac{8}{13}$ ($\sim 60\%$) cline studies and $\frac{7}{18}$ ($\sim 40\%$) model-based studies do so. Note, however, that there may be an additional influence of the sampling size, as model-based surveys are enriched with uninformative sampling designs, i.e. many individuals but few loci (Wang and Hey, 2010); and this factor may partly explain the lack of consensus across methods.

Critically, the empirical testing of our theoretical predictions may be impeded by the weak impact of sex chromosome linkage, dosage compensation and sex bias on the capacity of sex chromosomes to better resist to interspecies introgression. Actually, the main determinant of the barrier strength between species remains the genetic architecture of reproductive isolation (i.e., the number of barrier loci and their level of recessivity and/or epistasis); but, whether or not it differs between sex chromosomes and autosomes remains an open question. Finally, our predictions (which rely on the crucial assumption of rare introgression) may not fully apply to these empirical studies where the frequency of introgressing alleles must be high enough if they are to be detected.

3. Limitations of the model

The present model asks whether the chromosomal location of reproductive barriers (i.e., sex chromosomes vs. autosomes) influences their capacity to impede interspecies genetic exchange, and ultimately, promote or undermine speciation. Nevertheless, the rate of accumulation of barrier loci during species divergence may also vary with chromosomal location. The "faster-X theory" (Charlesworth et al., 1987) proposes that if most incompatible alleles between species first arise from advantageous recessive mutations within species, then they should accumulate more rapidly on the sex chromosome (where their effects are immediately exposed to selection in the heterogametic sex) relative to autosomes. If this theory is true, then sex chromosomes are expected to evolve more rapidly than autosomes, and as a result, are expected to form stronger interspecific barriers. However, the empirical evidence in favour of a greater efficacy of selection on the sex chromosome remains inconclusive (Meisel and Connallon, 2013). A reason is that the theory is based on many assumptions, including that mutations should be at least partially recessive, that the effective size of the sex chromosome is at least $\frac{3}{4}$ that of the autosomes, and that adaptation comes from *denovo* mutations (and not from standing genetic variation; Orr and Betancourt, 2001).

Another caveat is that most studies uses a metric that confuses adaptive and non-adaptive causes of the "faster-X effect"; in other words, the faster molecular rate of sex chromosomes may be either due to a higher rate of fixation of advantageous mutations or to a lower rate of fixation of weakly deleterious mutations. A much less widely used approach, requiring the acquisition of polymorphism data (Smith and Eyre-Walker, 2002), allows the contribution of these two classes of mutations to be distinguished. Applied to genomic data, it shows that mammalian species display a faster adaptive evolution of the X chromosome (*Oryctolagus cuniculus*: Carneiro et al., 2012; *Mus musculus*: Kousathanas et al., 2014; *Homo sapiens*: Veeramah et al., 2014), which may contribute to its enhanced barrier strength (Table 4). In *Drosophila*, conclusions are more conflicting, since some species display a faster-X adaptive rate while others do not (Charlesworth et al., 2018). In contrast, a faster accumulation of slightly deleterious mutations seems to be the major cause of faster-Z evolution in birds (Mank et al., 2010; Wright et al., 2015), as the higher variance in male reproductive success decreases the sex chromosome effective size well below the expected $\frac{3}{4}$ compared to autosomes, increasing the level of genetic drift. Relating these within-species evolutionary rates to the accumulation of barrier loci between species ultimately requires to understand the molecular basis of speciation (Presgraves, 2010), i.e. whether reproductive isolation mainly evolves as a by-product of adaptation or from non-adaptive processes (e.g., arm races between selfish genetic elements).

Our model of genetic exchange in a mainland-island setting rests on the assumptions that the rate of migration is small relative to selection, and so hybrids remain rare. However, to take into account the clinal structure of many hybrid zones (Barton and Hewitt, 1985) and their centre, where incompatible alleles are at an intermediate frequency; it will be necessary to extent our model to more realistic spatial structure, such as a stepping-stone model or a continuous habitat. This will require a different treatment outside the scope of the study, which takes into account the possibility of genomes with multiple introgressed blocks (see Barton (1983) and Barton and Bengtsson (1986)). Moreover, in this situation, dominance of the incompatible alleles will become important in the analytical treatment; and so deviations from the simple expectation that introgression in the sex-linked case is the same as introgression in the autosomal case with appropriately re-scaled parameters could arise.

Another assumption is that our model is deterministic, i.e. the population sizes are large enough that any effect of genetic drift can be neglected, which is of course unrealistic in most natural populations. Also, the outcomes of a hybridization event (where one or a few foreign genomes are introduced and randomly split by recombination) are largely stochastic (Baird et al., 2003). An extension of the model to include these stochastic processes will thus be necessary to understand the short-term evolution of hybrid genomes.

Our model assumes that the neutral marker is located at the end of the chromosome ("rod" model). A more general case would be to estimate the strength of a barrier generated by incompatible alleles onto the flow of a neutral marker embedded in the middle of the chromosome. Previous work on autosomes has shown that under this model the barrier is much stronger (Barton and Bengtsson, 1986), because two recombination events (instead of one) are required for the

neutral marker to escape; although this increase in barrier strength is much weaker when the neutral marker is not very close to the end of the chromosome. Importantly, we expect that the predictions concerning sex-linked barriers would again be obtained by using effective parameters; and so our general conclusions would hold regardless of the position of the neutral marker along the chromosome.

Another assumption is that all selected alleles are exclusively, and equally, deleterious in the recipient species. A more realistic model would be to consider allelic effects that vary along the chromosome (i.e., from globally adaptive to locally deleterious). Sachdeva and Barton (2018) developed a framework heading in that direction: they extended the infinitesimal model to take into account linkage between an infinite number of loci each having an infinitesimal effect (negative or positive) on a selected trait. Importantly, they demonstrated that the introgression dynamics of such a block is qualitatively different from introgression of blocks that carry purely deleterious variants: in that case, deleterious variants could attain high frequency in the recipient species *via* hitchhiking with genomic blocks with net positive effect (see also Bisschop et al., 2019 for a simulation study). Thus it would be informative to extend the present model to examine how hitchhiking with globally adaptive variants influences relative barrier strength of sex chromosomes vs autosomes.

Finally, we would also need to take into account the genome-wide reduction in the effective neutral gene flow due to loosely linked loci (which should affect different chromosomes in the same way), and would thus further reduce the difference between sex chromosomes and autosomes in species with large genomes.

Table 4. Studies testing whether the sex chromosome is a stronger barrier to gene flow than autosomes

Inferences are either based on (.) the migration rates under isolation-with-migration models (Sousa and Hey, 2013), (#) the number of introgressed tracts (Lawson et al., 2012), or (°) the geographic/genomic cline widths (Barton and Hewitt, 1985). We discarded studies only based on descriptive statistics such as FST (Weir and Cockerham, 1984), GMIN (Geneva et al., 2015) or f-statistics (Patterson et al., 2012). **AGE**: age of the sex chromosome (Filatov, 2005; Vicoso and Bachtrog, 2015; Miura, 2017; Vicoso, 2019). **DOSAGE**: dosage compensation mechanism (Gu and Walters, 2017; Hebbert, 1984). **SEX BIAS**: sex-biased forces among which the migration rate (m: Greenwood, 1980), the recombination rate (c: Lenormand and Dutheil (2005); Satomura et al. (2019)) and the sexual selection strength (s: Wilson Sayres, 2018). **INTROG**: if $X < A$ then the sex chromosome is a stronger barrier to gene flow than autosomes (either because it has a lower migration rate, a lower number of introgressed tract or steeper clines), $X \geq A$ otherwise. A **LOCUS** / X **LOCUS**: number of autosomal/X-linked loci available for the inferences. Studies with less than three loci available for sex chromosomes and/or autosomes were discarded.

XY SEXUAL SYSTEMS	FEATURES OF THE X		SEX BIAS			INFERENCE		
	AGE	DOSAGE	m	c	s	INTROG	A LOCUS	X LOCUS
Insects								
Orthoptera	-	yes	-	♂ ~ ♀	-			
°*Gryllus pennsylvanicus* / *G. firmus* (1)						$X < A$	genome-wide	genome-wide
Diptera	250 My	♂ over-regulation	-	♂ = 0	-			
#*Drosophila yakuba* / *D. santomea* (2)				yes		$X < A$	genome-wide	genome-wide
.*Drosophila melanogaster* EUR / AFR (3)				yes		$X \geq A$	genome-wide	genome-wide
.*Drosophila melanogaster* / *D. simulans* (4)				yes		$X \geq A$	genome-wide	genome-wide
.*Drosophila subquinaria* / *D. recens* (5)				?		$X \geq A$	19	7
.*Drosophila persimilis* / *D. pseudoobscura* (6)	neo-X			yes		$X \geq A$	genome-wide	genome-wide
.*Drosophila subobscura* / *D. madeirensis* (7)	=			yes		$X \geq A$	16	3
.*Drosophila athabasca* WEST / EAST (8)	10 My			yes		$X \geq A$	genome-wide	genome-wide
Mammals	150 My	♀ inactivation	♂ > ♀	♀ > ♂	♂ > ♀	-	-	-
Primates								
#*Homo sapiens* / *H. neanderthalensis* (9)						$X < A$	genome-wide	genome-wide
°*Alouatta palliata* / *A. nigra* (10)						$X \geq A$	genome-wide	genome-wide
Rodentia								
°*Mus m. musculus* / *Mus m. domesticus* (11)						$X < A$	genome-wide	genome-wide
#*Mus m. domesticus* / *Mus spretus* (12)						$X < A$	genome-wide	genome-wide
Lagomorpha								
°*Oryctolagus c. cuniculus* / *O. c. algirus* (13)						$X < A$	genome-wide	genome-wide
Amphibians								
Anura	recent	needless	-	♀ > ♂	-	-	-	-
°*Hyla arborea* / *H. orientalis* (14)						$X < A$	21	8
°*Bufo viridis* / *B. balearicus*						$X \geq A$	17	10
/ *B. siculus* (15)							14	12
Plants								
Caryophyllales	10 My	♂ over-regulation	-	-	-	-	-	-
.*Silene latifolia* / *S. dioica* (16)						$X < A$	genome-wide	genome-wide

(1) Larson et al., 2014; (2) Turissini and Matute, 2017; (3) Kapopoulou et al., 2018; (4) Dalquen et al., 2017; (5) Ginsberg et al., 2019; (6) Fuller et al., 2018; (7) Herrig et al., 2014; (8) Wong Miller et al., 2017; (9) Steinrücken et al., 2018; (10) Baiz et al., 2019; (11) Wang et al., 2011; (12) Liu et al., 2015; (13) Carneiro et al., 2010; Rafati et al., 2018; (14) Dufresnes et al., 2016; (15) Gerchen et al., 2018; (16) Hu and Filatov, 2016

ZW SEXUAL SYSTEMS	FEATURES OF THE Z		SEX BIAS			INFERENCE		
	AGE	DOSAGE	m	c	s	INTROG	A LOCUS	X LOCUS
Birds	**100 My**	**no**	♀ > ♂	♂ ~ ♀	♂ > ♀	-	-	-
Accipitriformes								
.*Aquila clanga* / *A. pomarina* (17)						$X < A$	36	15
Anseriformes								
.*Anas castanea* / *A. gracilis* (18)						$X \geq A$	17	7
Galliformes								
.*Tympanuchus cupido* / *T. pallidicinctus* / *T. phasianellus* (19)						$X < A$	4	5
Pelecaniformes								
.*Sula nebouxii* / *S. variegata* (20)						$X \geq A$	4	3
°*Plegadis falcinellus* / *P. chihi* (21)						$X \geq A$	genome-wide	genome-wide
Piciformes								
°*Picus v. viridis* / *P. sharpei* (22)						$X \geq A$	9	10
Passeriformes								
.*Zosterops borbonicus* LOW / HIGH (23)						$X < A$	genome-wide	genome-wide
.*Passerina amoena* / *P. cyanea* (24)						$X < A$	13	6
°*Passer domesticus* / *P. hispaniolensis* (25)						$X < A$	genome-wide	genome-wide
°*Poephila acuticauda* / *P. cincta* (26)						$X < A$	genome-wide	genome-wide
°*Poecile atricapillus* / *P. carolinensis* (27)						$X < A$	genome-wide	genome-wide
.*Certhia americana* SOU / NOR (28)						$X < A$	21	9
.*Luscinia luscinia* / *L. megarhynchos* (29)						$X < A$	8	4
.*Ficedula albicollis* / *F. hypoleuca* (30)						$X \geq A$	6	5
.*Carpodacus vinaceus* / *C. formosanus* (31)						$X \geq A$	25	10
.*Aegithalos bonvaloti* / *A. fuliginosus* (32)						$X \geq A$	3	3
°*Corvus c. corone* / *C. c. cornix* (33)						$X \geq A$	genome-wide	genome-wide
Insects								
Lepidoptera	**250 My**	**♂ under-regulation**	-	♀ = 0	-	-	-	-
°*Papilio glaucus* / *P. canadensis* (34)				?		$X < A$	genome-wide	genome-wide

(17) Backström and Väli, 2011; (18) Dhami et al., 2016; (19) Galla and Johnson, 2015; (20) Taylor et al., 2013; (21) Oswald et al., 2019; (22) Pons et al., 2019; (23) Bourgeois et al., 2018; (24) Carling et al., 2010; (25) Trier et al., 2014; (26) Hooper et al., 2019; (27) Taylor et al., 2014; (28) Manthey and Spellman, 2014; (29) Storchová et al., 2010; (30) Hogner et al., 2012; (31) Chu et al., 2013; (32) Wang et al., 2014; (33) Knief et al., 2019; (34) Ryan et al., 2017

Data accessibility

SLiM simulation codes and Mathematica notebooks are available on [[to be uploaded on a public repository as Dryad]].

Author contributions

C.F. designed the project, C.F. and H. S. derived the analytical and numerical results, C.F. conducted the simulations. C.F. and H.S. wrote the manuscript.

Acknowledgements

CF was supported by an Austrian Science Foundation FWF grant (Project M 2463-B29). The computations were performed with the IST Austria High-Performance Computing (HPC) Cluster and the Institut Français de Bioinformatique

(IFB) Core Cluster. We are grateful to Nick Barton and Beatriz Vicoso for critical comments on the manuscript; and we also thank Nick Barton for insightful suggestions on the model.

References

Bachtrog, D., S. Mahajan, and R. Bracewell
2019. Massive gene amplification on a recently formed drosophila y chromosome. *Nature ecology & evolution*, 3(11):1587–1597.

Bachtrog, D., J. E. Mank, C. L. Peichel, M. Kirkpatrick, S. P. Otto, T.-L. Ashman, M. W. Hahn, J. Kitano, I. Mayrose, R. Ming, et al.
2014. Sex determination: why so many ways of doing it? *PLoS Biol*, 12(7):e1001899.

Backström, N. and Ü. Väli
2011. Sex- and species- biased gene flow in a spotted eagle hybrid zone. *BMC evolutionary biology*, 11(1):100.

Baird, S., N. Barton, and A. Etheridge
2003. The distribution of surviving blocks of an ancestral genome. *Theoretical population biology*, 64(4):451–471.

Baiz, M. D., P. K. Tucker, and L. Cortés-Ortiz
2019. Multiple forms of selection shape reproductive isolation in a primate hybrid zone. *Molecular ecology*, 28(5):1056–1069.

Barton, N.
1983. Multilocus clines. *Evolution*, 37(3):454–471.

Barton, N. and B. O. Bengtsson
1986. The barrier to genetic exchange between hybridising populations. *Heredity*, 57(3):357–376.

Barton, N. H.
1995. Linkage and the limits to natural selection. *Genetics*, 140(2):821–841.

Barton, N. H. and G. M. Hewitt
1985. Analysis of hybrid zones. *Annual review of Ecology and Systematics*, 16(1):113–148.

Bengtsson, B. O.
1985. *The flow of genes through a genetic barrier in Evolution: essays in honour of John Maynard Smith*. Cambridge University Press.

Bisschop, G., D. Setter, M. Rafajlovic, S. J. Baird, and K. Lohse
2019. The impact of global selection on local adaptation and reproductive isolation. *bioRxiv*, P. 855320.

Bourgeois, Y. X., J. A. Bertrand, B. Delahaie, H. Holota, C. Thébaud, and B. Milá
2018. Local adaptation and sexual selection drive intra-island diversification in a songbird lineage: differential divergence in autosomes and sex chromosomes. *bioRxiv*.

Carling, M. D., I. J. Lovette, and R. T. Brumfield
2010. Historical divergence and gene flow: coalescent analyses of mitochondrial, autosomal and sex-linked loci in passerina buntings. *Evolution: International Journal of Organic Evolution*, 64(6):1762–1772.

Carneiro, M., F. W. Albert, J. Melo-Ferreira, N. Galtier, P. Gayral, J. A. Blanco-Aguiar, R. Villafuerte, M. W. Nachman, and N. Ferrand
2012. Evidence for widespread positive and purifying selection across the european rabbit (oryctolagus cuniculus) genome. *Molecular biology and evolution*, 29(7):1837–1849.

Carneiro, M., J. A. Blanco-Aguiar, R. Villafuerte, N. Ferrand, and M. W. Nachman
2010. Speciation in the european rabbit (oryctolagus cuniculus): islands of differentiation on the x chromosome and autosomes. *Evolution: International Journal of Organic Evolution*, 64(12):3443–3460.

Cattani, M. V. and D. C. Presgraves
2012. Incompatibility between x chromosome factor and pericentric heterochromatic region causes lethality in hybrids between drosophila melanogaster and its sibling species. *Genetics*, 191(2):549–559.

Charlesworth, B., J. L. Campos, and B. C. Jackson
2018. Faster-x evolution: Theory and evidence from drosophila. *Molecular ecology*, 27(19):3753–3771.

Charlesworth, B., J. A. Coyne, and N. H. Barton
1987. The relative rates of evolution of sex chromosomes and autosomes. *The American Naturalist*, 130(1):113–146.

Chu, J.-H., D. Wegmann, C.-F. Yeh, R.-C. Lin, X.-J. Yang, F.-M. Lei, C.-T. Yao, F.-S. Zou, and S.-H. Li
2013. Inferring the geographic mode of speciation by contrasting autosomal and sex-linked genetic diversity. *Molecular biology and evolution*, 30(11):2519–2530.

Coyne, J. and A. H. Orr
1989. *Two rules of speciation in Speciation and its consequences*. Sinauer Associates.

Cruickshank, T. E. and M. W. Hahn
2014. Reanalysis suggests that genomic islands of speciation are due to reduced diversity, not reduced gene flow. *Molecular ecology*, 23(13):3133–3157.

Dalquen, D. A., T. Zhu, and Z. Yang
2017. Maximum likelihood implementation of an isolation-with-migration model for three species. *Systematic Biology*, 66(3):379–398.

Deakin, J. E., J. Chaumeil, T. A. Hore, and J. A. M. Graves
2009. Unravelling the evolutionary origins of x chromosome inactivation in mammals: insights from marsupials and monotremes. *Chromosome Research*, 17(5):671–685.

Dhami, K. K., L. Joseph, D. A. Roshier, and J. L. Peters
2016. Recent speciation and elevated z-chromosome differentiation between sexually monochromatic and dichromatic species of australian teals. *Journal of Avian Biology*, 47(1):92–102.

Dobzhansky, T. H.
1936. Studies on hybrid sterility. ii. localization of sterility factors in drosophila pseudoobscura hybrids. *Genetics*, 21(2):113.

Dobzhansky, T. H.
1937. *Genetics and the origin of species*. Colombia U.P.

Dufresnes, C., T. Majtyka, S. J. Baird, J. F. Gerchen, A. Borzée, R. Savary, M. Ogielska, N. Perrin, and M. Stöck
2016. Empirical evidence for large x-effects in animals with undifferentiated sex chromosomes. *Scientific reports*, 6(1):1–7.

Ellegren, H., L. Hultin-Rosenberg, B. Brunström, L. Dencker, K. Kultima, and B. Scholz
2007. Faced with inequality: chicken do not have a general dosage compensation of sex-linked genes. *BMC biology*, 5(1):40.

Ellegren, H. and J. Parsch
2007. The evolution of sex-biased genes and sex-biased gene expression. *Nature Reviews Genetics*, 8(9):689–698.

Filatov, D. A.
2005. Evolutionary history of silene latifolia sex chromosomes revealed by genetic mapping of four genes. *Genetics*, 170(2):975–979.

Filatov, D. A.
2018. The two ârules of speciationâ in species with young sex chromosomes. *Molecular ecology*, 27(19):3799–3810.

Fraïsse, C., J. Elderfield, and J. Welch
2014. The genetics of speciation: are complex incompatibilities easier to evolve? *Journal of evolutionary biology*, 27(4):688–699.

Frank, S. A.
1991. Divergence of meiotic drive-suppression systems as an explanation for sex-biased hybrid sterility and inviability. *Evolution*, 45(2):262–267.

Fuller, Z. L., C. J. Leonard, R. E. Young, S. W. Schaeffer, and N. Phadnis
2018. Ancestral polymorphisms explain the role of chromosomal inversions in speciation. *PLoS genetics*, 14(7):e1007526.

Galla, S. J. and J. A. Johnson
2015. Differential introgression and effective size of marker type influence phylogenetic inference of a recently divergent avian group (phasianidae: Tympanuchus). *Molecular phylogenetics and evolution*, 84:1–13.

Geneva, A. J., C. A. Muirhead, S. B. Kingan, and D. Garrigan
2015. A new method to scan genomes for introgression in a secondary contact model. *PloS one*, 10(4).

Gerchen, J. F., C. Dufresnes, and M. Stöck
2018. Introgression across hybrid zones is not mediated by large x-effects in green toads with undifferentiated sex chromosomes. *The American Naturalist*, 192(5):E178–E188.

Ginsberg, P. S., D. P. Humphreys, and K. A. Dyer
2019. Ongoing hybridization obscures phylogenetic relationships in the drosophila subquinaria species complex. *Journal of Evolutionary Biology*, 32(10):1093–1105.

Greenwood, P. J.
1980. Mating systems, philopatry and dispersal in birds and mammals. *Animal behaviour*, 28(4):1140–1162.

Gu, L. and J. R. Walters
2017. Evolution of sex chromosome dosage compensation in animals: a beautiful theory, undermined by facts and bedeviled by details. *Genome biology and evolution*, 9(9):2461–2476.

Haldane, J. B. S.
1922. Sex ratio and unisexual sterility in hybrid animals. *Journal of Genetics*, 12(2):101–109.

Haller, B. C. and P. W. Messer
2019. Slim 3: forward genetic simulations beyond the wright–fisher model. *Molecular biology and evolution*, 36(3):632–637.

Hebbert, D. R.
1984. Dosage compensation of the sex-linked enzyme phosphoglucomutase in the orthoptera. *Heredity*, 53(2):361–369.

Hedrick, P. W.
2007. Sex: differences in mutation, recombination, selection, gene flow, and genetic drift. *Evolution: International Journal of Organic Evolution*, 61(12):2750–2771.

Herrig, D. K., A. J. Modrick, E. Brud, and A. Llopart
2014. Introgression in the drosophila subobscuraâd. madeirensis sister species: evidence of gene flow in nuclear genes despite mitochondrial differentiation. *Evolution*, 68(3):705–719.

Hewitt, G.
2000. The genetic legacy of the quaternary ice ages. *Nature*, 405(6789):907–913.

Hoellinger, I. and J. Hermisson
2017. Bounds to parapatric speciation: a dobzhansky–muller incompatibility model involving autosomes, x chromosomes, and mitochondria. *Evolution*, 71(5):1366–1380.

Hogner, S., S. A. Sæther, T. Borge, T. Bruvik, A. Johnsen, and G.-P. Sætre
2012. Increased divergence but reduced variation on the z chromosome relative to autosomes in ficedula flycatchers: differential introgression or the faster-z effect? *Ecology and evolution*, 2(2):379–396.

Hooper, D. M., S. C. Griffith, and T. D. Price
2019. Sex chromosome inversions enforce reproductive isolation across an avian hybrid zone. *Molecular ecology*, 28(6):1246–1262.

Hu, X.-S. and D. A. Filatov
2016. The large-x effect in plants: increased species divergence and reduced gene flow on the silene x-chromosome. *Molecular ecology*, 25(11):2609–2619.

Hurst, L. D. and A. Pomiankowski
1991. Causes of sex ratio bias may account for unisexual sterility in hybrids: a new explanation of haldane's rule and related phenomena. *Genetics*, 128(4):841–858.

Hvala, J. A., M. E. Frayer, and B. A. Payseur
2018. Signatures of hybridization and speciation in genomic patterns of ancestry. *Evolution*, 72(8):1540–1552.

Kapopoulou, A., M. Kapun, P. Pavlidis, B. Pieper, R. Wilches, W. Stephan, and S. Laurent
2018. Early split between african and european populations of drosophila melanogaster. *bioRxiv*.

Knief, U., C. M. Bossu, N. Saino, B. Hansson, J. Poelstra, N. Vijay, M. Weissensteiner, and J. B. Wolf
2019. Epistatic mutations under divergent selection govern phenotypic variation in the crow hybrid zone. *Nature ecology & evolution*, 3(4):570–576.

Kousathanas, A., D. L. Halligan, and P. D. Keightley
2014. Faster-x adaptive protein evolution in house mice. *Genetics*, 196(4):1131–1143.

Larson, E. L., T. A. White, C. L. Ross, and R. G. Harrison
2014. Gene flow and the maintenance of species boundaries. *Molecular Ecology*, 23(7):1668–1678.

Lawson, D. J., G. Hellenthal, S. Myers, and D. Falush
2012. Inference of population structure using dense haplotype data. *PLoS genetics*, 8(1).

Lenormand, T. and J. Dutheil
2005. Recombination difference between sexes: a role for haploid selection. *PLoS biology*, 3(3).

Lima, T. G.
2014. Higher levels of sex chromosome heteromorphism are associated with markedly stronger reproductive isolation. *Nature Communications*, 5(1):1–8.

Lindtke, D. and C. A. Buerkle
2015. The genetic architecture of hybrid incompatibilities and their effect on barriers to introgression in secondary contact. *Evolution*, 69(8):1987–2004.

Liu, K. J., E. Steinberg, A. Yozzo, Y. Song, M. H. Kohn, and L. Nakhleh
2015. Interspecific introgressive origin of genomic diversity in the house mouse. *Proceedings of the National Academy of Sciences*, 112(1):196–201.

Llopart, A., E. Brud, N. Pettie, and J. M. Comeron
2018. Support for the dominance theory in drosophila transcriptomes. *Genetics*, 210(2):703–718.

Maheshwari, S. and D. A. Barbash
2011. The genetics of hybrid incompatibilities. *Annual review of genetics*, 45:331–355.

Mank, J. E.
2013. Sex chromosome dosage compensation: definitely not for everyone. *Trends in genetics*, 29(12):677–683.

Mank, J. E., B. Vicoso, S. Berlin, and B. Charlesworth
2010. Effective population size and the faster-x effect: Empirical results and their interpretation. *Evolution: International Journal of Organic Evolution*, 64(3):663–674.

Manthey, J. D. and G. M. Spellman
2014. Increased differentiation and reduced gene flow in sex chromosomes relative to autosomes between lineages of the brown creeper certhia americana. *Journal of avian biology*, 45(2):149–156.

Matsubara, K., E. Yamamoto, R. Mizobuchi, J.-i. Yonemaru, T. Yamamoto, H. Kato, and M. Yano
2015. Hybrid breakdown caused by epistasis-based recessive incompatibility in a cross of rice (oryza sativa l.). *Journal of Heredity*, 106(1):113–122.

Meisel, R. P. and T. Connallon
2013. The faster-x effect: integrating theory and data. *Trends in genetics*, 29(9):537–544.

Miura, I.
2017. Sex determination and sex chromosomes in amphibia. *Sexual Development*, 11(5-6):298–306.

Muirhead, C. A. and D. C. Presgraves
2016. Hybrid incompatibilities, local adaptation, and the genomic distribution of natural introgression between species. *The American Naturalist*, 187(2):249–261.

Muller, H. J.
1940. *Bearing of the Drosophila work on systematics in The New Systematics*. Clarendon Press.

Nei, M. and W.-H. Li
1979. Mathematical model for studying genetic variation in terms of restriction endonucleases. *Proceedings of the National Academy of Sciences*, 76(10):5269–5273.

Orr, H. A. and A. J. Betancourt
2001. Haldane's sieve and adaptation from the standing genetic variation. *Genetics*, 157(2):875–884.

Oswald, J. A., M. G. Harvey, R. C. Remsen, D. U. Foxworth, D. L. Dittmann, S. W. Cardiff, and R. T. Brumfield
2019. Evolutionary dynamics of hybridization and introgression following the recent colonization of glossy ibis (aves: Plegadis falcinellus) into the new world. *Molecular ecology*, 28(7):1675–1691.

Patterson, N., P. Moorjani, Y. Luo, S. Mallick, N. Rohland, Y. Zhan, T. Genschoreck, T. Webster, and D. Reich
2012. Ancient admixture in human history. *Genetics*, 192(3):1065–1093.

Payseur, B. A., D. C. Presgraves, and D. A. Filatov
2018. Sex chromosomes and speciation. *Molecular ecology*, 27(19):3745.

Pons, J.-M., C. Masson, G. Olioso, and J. Fuchs
2019. Gene flow and genetic admixture across a secondary contact zone between two divergent lineages of the eurasian green woodpecker picus viridis. *Journal of Ornithology*, 160(4):935–945.

Presgraves, D. C.
2010. The molecular evolutionary basis of species formation. *Nature Reviews Genetics*, 11(3):175–180.

Presgraves, D. C.
2018. Evaluating genomic signatures of âthe large x-effectâ during complex speciation. *Molecular ecology*, 27(19):3822–3830.

R, C.
2013. R: A language and environment for statistical computing.

Rafati, N., J. A. Blanco-Aguiar, C. J. Rubin, S. Sayyab, S. J. Sabatino, S. Afonso, C. Feng, P. C. Alves, R. Villafuerte, N. Ferrand, et al.
2018. A genomic map of clinal variation across the european rabbit hybrid zone. *Molecular ecology*, 27(6):1457–1478.

Roux, C., C. Fraisse, J. Romiguier, Y. Anciaux, N. Galtier, and N. Bierne
2016. Shedding light on the grey zone of speciation along a continuum of genomic divergence. *PLoS biology*, 14(12).

Roux, C., G. Tsagkogeorga, N. Bierne, and N. Galtier
2013. Crossing the species barrier: genomic hotspots of introgression between two highly divergent ciona intestinalis species. *Molecular biology and evolution*, 30(7):1574–1587.

Ryan, S. F., M. C. Fontaine, J. M. Scriber, M. E. Pfrender, S. T. O'Neil, and J. J. Hellmann
2017. Patterns of divergence across the geographic and genomic landscape of a butterfly hybrid zone associated with a climatic gradient. *Molecular ecology*, 26(18):4725–4742.

Sachdeva, H. and N. H. Barton
2018. Introgression of a block of genome under infinitesimal selection. *Genetics*, 209(4):1279–1303.

Satomura, K., N. Osada, and T. Endo
2019. Achiasmy and sex chromosome evolution. *Ecological Genetics and Genomics*, P. 100046.

Schilthuizen, M., M. Giesbers, and L. Beukeboom
2011. Haldane's rule in the 21st century. *Heredity*, 107(2):95–102.

Sciuchetti, L., C. Dufresnes, E. Cavoto, A. Brelsford, and N. Perrin
2018. Dobzhansky–muller incompatibilities, dominance drive, and sex-chromosome introgression at secondary contact zones: A simulation study. *Evolution*, 72(7):1350–1361.

Sethuraman, A., V. Sousa, and J. Hey
2019. Model-based assessments of differential introgression and linked natural selection during divergence and speciation. *bioRxiv*.

Smith, N. G. and A. Eyre-Walker
2002. Adaptive protein evolution in drosophila. *Nature*, 415(6875):1022–1024.

Sousa, V. and J. Hey
2013. Understanding the origin of species with genome-scale data: modelling gene flow. *Nature Reviews Genetics*, 14(6):404–414.

Steinrücken, M., J. P. Spence, J. A. Kamm, E. Wieczorek, and Y. S. Song
2018. Model-based detection and analysis of introgressed neanderthal ancestry in modern humans. *Molecular ecology*, 27(19):3873–3888.

Storchová, R., J. Reif, and M. W. Nachman
2010. Female heterogamety and speciation: reduced introgression of the z chromosome between two species of nightingales. *Evolution: International Journal of Organic Evolution*, 64(2):456–471.

Taylor, S. A., D. J. Anderson, and V. L. Friesen
2013. Evidence for asymmetrical divergence-gene flow of nuclear loci, but not mitochondrial loci, between seabird sister species: Blue-footed (sula nebouxii) and peruvian (s. variegata) boobies. *PloS one*, 8(4).

Taylor, S. A., R. L. Curry, T. A. White, V. Ferretti, and I. Lovette
2014. Spatiotemporally consistent genomic signatures of reproductive isolation in a moving hybrid zone. *Evolution*, 68(11):3066–3081.

Trier, C. N., J. S. Hermansen, G.-P. Sætre, and R. I. Bailey
2014. Evidence for mito-nuclear and sex-linked reproductive barriers between the hybrid italian sparrow and its parent species. *PLoS genetics*, 10(1).

Turelli, M. and H. A. Orr
1995. The dominance theory of haldane's rule. *Genetics*, 140(1):389–402.

Turelli, M. and H. A. Orr
2000. Dominance, epistasis and the genetics of postzygotic isolation. *Genetics*, 154(4):1663–1679.

Turissini, D. A. and D. R. Matute
2017. Fine scale mapping of genomic introgressions within the drosophila yakuba clade. *PLoS genetics*, 13(9):e1006971.

Veeramah, K. R., R. N. Gutenkunst, A. E. Woerner, J. C. Watkins, and M. F. Hammer
2014. Evidence for increased levels of positive and negative selection on the x chromosome versus autosomes in humans. *Molecular biology and evolution*, 31(9):2267–2282.

Vicoso, B.
2019. Molecular and evolutionary dynamics of animal sex-chromosome turnover. *Nature ecology & evolution*, Pp. 1–10.

Vicoso, B. and D. Bachtrog
2015. Numerous transitions of sex chromosomes in diptera. *PLoS biology*, 13(4).

Wang, L., K. Luzynski, J. E. Pool, V. Janoušek, P. Dufková, M. M. Vyskočilová, K. C. Teeter, M. W. Nachman, P. Munclinger, M. Macholán, et al.
2011. Measures of linkage disequilibrium among neighbouring snps indicate asymmetries across the house mouse hybrid zone. *Molecular ecology*, 20(14):2985–3000.

Wang, R.-X.
2013. Gene flow across a hybrid zone maintained by a weak heterogametic incompatibility and positive selection of incompatible alleles. *Journal of evolutionary biology*, 26(2):386–398.

Wang, W., C. Dai, P. Alström, C. Zhang, Y. Qu, S.-H. Li, X. Yang, N. Zhao, G. Song, and F. Lei
2014. Past hybridization between two east asian long-tailed tits (aegithalos bonvaloti and a. fuliginosus). *Frontiers in zoology*, 11(1):40.

Wang, Y. and J. Hey
2010. Estimating divergence parameters with small samples from a large number of loci. *Genetics*, 184(2):363–379.

Weir, B. S. and C. C. Cockerham
1984. Estimating f-statistics for the analysis of population structure. *Evolution*, 38(6):1358–1370.

Wilkinson-Herbots, H. M.
2008. The distribution of the coalescence time and the number of pairwise nucleotide differences in the âisolation with migrationâ model. *Theoretical population biology*, 73(2):277–288.

Wilson Sayres, M. A.
2018. Genetic diversity on the sex chromosomes. *Genome biology and evolution*, 10(4):1064–1078.

Wong Miller, K. M., R. R. Bracewell, M. B. Eisen, and D. Bachtrog
2017. Patterns of genome-wide diversity and population structure in the drosophila athabasca species complex. *Molecular biology and evolution*, 34(8):1912–1923.

Wright, A. E., P. W. Harrison, F. Zimmer, S. H. Montgomery, M. A. Pointer, and J. E. Mank
2015. Variation in promiscuity and sexual selection drives avian rate of faster-z evolution. *Molecular ecology*, 24(6):1218–1235.

Wu, C.-I.
2001. The genic view of the process of speciation. *Journal of evolutionary biology*, 14(6):851–865.